available at www.sciencedirect.com

ScienceDirect

www.elsevier.com/locate/yclim
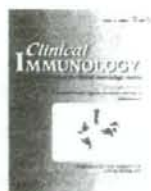
Clinical IMMUNOLOGY

Disruption of Nrf2 enhances susceptibility to airway inflammatory responses induced by low-dose diesel exhaust particles in mice

Ying Ji Li [a,d], Hajime Takizawa [b], Arata Azuma [c], Tadashi Kohyama [e], Yasuhiro Yamauchi [e], Satoru Takahashi [f], Masayuki Yamamoto [f], Tomoyuki Kawada [a], Shoji Kudoh [c], Isamu Sugawara [d,*]

[a] Department of Hygiene and Public Health, Nippon Medical School, Tokyo, Japan
[b] Fourth Department of Internal Medicine, Teikyo University, School of Medicine, Kawasaki, Japan
[c] Department of Pulmonary Medicine/Infection and Oncology, Nippon Medical School, Tokyo, Japan
[d] Mycobacterial Reference Center, The Research Institute of Tuberculosis, Kiyose, Japan
[e] Department of Respiratory Medicine, University of Tokyo, School of Medicine, Tokyo, Japan
[f] Institute of Basic Medical Sciences, University of Tsukuba, Ibaragi, Japan

Abstract   To test our hypothesis that diesel exhaust particle (DEP)-induced oxidative stress and host antioxidant responses play a key role in the development of DEP-induced airway inflammatory diseases, C57BL/6 nuclear erythroid 2 P45-related factor 2 (Nrf2) knockout ($Nrf2^{-/-}$) and wild-type mice were exposed to low-dose DEP for 7 h/day, 5 days/week, for 8 weeks. $Nrf2^{-/-}$ mice exposed to low-dose DEP showed significantly increased airway hyperresponsiveness and counts of lymphocytes and eosinophils, together with increased concentrations of IL-12 and IL-13, and thymus and activation-regulated chemokine (TARC), in BAL fluid than wild-type mice. In contrast, expression of antioxidant enzyme genes was significantly higher in wild-type mice than in $Nrf2^{-/-}$ mice. We have first demonstrated that disruption of Nrf2 enhances susceptibility to airway inflammatory responses induced by inhalation of low-dose DEP in mice. These results strongly suggest that DEP-induced oxidative stress and host antioxidant responses play some role in the development of DEP-induced airway inflammation.
© 2008 Elsevier Inc. All rights reserved.

Introduction

Air pollution is associated with increased mortality and morbidity. Although air pollutants include both gaseous components

* Corresponding author. Fax: +81 424 92 4600.
  E-mail address: sugawara@jata.or.jp (I. Sugawara).

(ozone, carbon monoxide, sulfur dioxide, and nitrogen dioxide) and particulate components, it has been shown that particulates, particularly PM10 (particulate matter with diameter less than 10 μm), are more relevant to many disorders. Currently, much attention is being focused on PM2.5 in relation to adverse health effects. Diesel exhaust particles (DEP) are the major component of PM2.5, and therefore the relationship between PM2.5 or PM10 and some diseases has been investigated

intensively [1–5]. The roles of reactive oxygen species (ROS) generated by exposure to DEP and the subsequent generation of the oxidative stress response have been emphasized through *in vitro* experimental studies [6–11]. These findings suggest that DEP induce activation of transcription factors and that ROS may play an important role in these processes. Thus, imbalance between oxygen stress/proinflammatory proteins and antioxidant proteins may be a key player in the development of hazardous effects. However, it is still not fully clear whether oxidative stress caused by inhalation of DEP leads to airway inflammation and airway hyperresponsiveness *in vivo*.

We have shown previously that continuous low-level exposure to DEP (100 μg/m^3 for 7 h/day, 5 days/week) significantly augments AHR and Th2-type cytokine/chemokine gene expression in murine asthma models [12]. Studies using two different mouse strains have demonstrated a difference in susceptibility to DEP exposure between them, and suggested that certain antioxidant enzymes may play an important role in susceptibility, C57BL/6 mice being more sensitive to low-dose DEP exposure than BALB/c mice [13,14].

Nuclear erythroid 2 P45-related factor 2 (Nrf2) is a redox-sensitive basic leucine zipper transcription factor that is involved in the transcriptional regulation of many antioxidant genes. The Nrf2-regulated genes in the lungs include almost all of the relevant antioxidant enzymes, such as HO-1 and several members of the GST family [15]. Therefore, to clarify whether or not oxidative stress and host antioxidant defenses play a central role in the pathogenesis of lung disease, several disease models using Nrf2$^{-/-}$ mice have been studied, including ovalbumin (OVA)-induced asthma [16], bleomycin-induced lung fibrosis [17], and cigarette smoke-induced emphysema [18]. It is reported that oxidative stress is involved in the development of DEP-induced airway inflammation [6–11] and that Nrf2 is also a key transcription factor that regulates antioxidant and defense action against the proinflammatory and oxidizing effects of DEP *in vitro* [9,11]. Furthermore, DNA adduct formation has been shown to be accelerated in the lungs of Nrf2$^{-/-}$ mice exposed to DEP (3 mg/m^3 for 4 weeks) [19]. However, no study has yet utilized Nrf2$^{-/-}$ mice to examine the pathogenesis of airway inflammation induced by low-dose DEP.

To test the hypothesis that DEP-induced oxidative stress and host antioxidant responses play a key role in the development of DEP-induced airway inflammatory disease *in vivo*, we conducted the present study using C57BL/6 Nrf2$^{-/-}$ and Nrf2$^{+/+}$ mice, and examined airway inflammatory responses and host antioxidant responses to low-dose DEP (i.e., at concentrations similar to those inhaled outdoors) exposure.

Materials and methods

Animals

Nrf2-deficient C57BL/6 mice were generated as described by Itoh et al. [20]. Mice were genotyped for Nrf2 status by PCR amplification of genomic DNA extracted from the tail [21]. PCR amplification was performed using three different primers:

Nrf2-sense for both genotypes: 5'-TGGACGGGACTATT-GAAGGCTG-3'

Nrf2-antisense for wild-type mice: 5'-GCCGCCTTTTCAG-TAGATGGAGG-3'
Nrf2-antisense for LacZ: 5'-GCGGATTGACCGTAATGGGA-TAGG-3'.

Amplification was performed using 30 cycles of 96 °C 20 s, 59 °C 30 s, and 72 °C 45 s. The wild-type allele produces a 734-bp band, while the knockout allele produces a 449-bp band. Mice were housed under specific pathogen-free (SPF) conditions with controlled temperature and lighting (23 ± 2 °C, 12 h light/dark periods). Age-matched 6-week-old female mice from the same litter were placed into chambers under same controlled conditions and exposed to DEP. All procedures conformed to the National Institutes of Health (NIH) guidelines for the care and use of laboratory animals.

DEP exposure

The *in vivo* DEP exposure system has been described previously [22,23]. The concentration of DEP was monitored and kept low (approximately 100 μg/m^3). C57BL/6 Nrf2$^{-/-}$ and Nrf2$^{+/+}$ mice were exposed to DEP for 7 h daily, 5 days a week.

Experimental protocol

Nrf2$^{-/-}$ and Nrf2$^{+/+}$ C57BL/6 mice were exposed to low-dose DEP or clean air (SPF) for 8 weeks. AHR was measured in all experimental groups immediately, and mice were sacrificed on day 56 of exposure to DEP or clean air in all experimental groups. We examined the histopathology of the lung tissues and the cell populations in BAL fluid. We also measured the concentrations of inflammatory cytokines and chemokines in the BAL fluid and the IgE, IgG$_1$ and IgG$_{2a}$ levels in the serum. We also examined the gene expression of antioxidants in the lung tissues.

Determination of AHR

Airway hyperresponsiveness was assessed by whole-body plethysmography with a free-moving application (Buxco Electronics, Troy, NY) [24] in accordance with a previously published procedure [12,13].

Histological analysis

For histologic examination, 10% formalin-fixed lung tissues were embedded in paraffin, cut into sections, and stained with hematoxylin and eosin (HE), and periodic acid-Schiff (PAS). Histopathological changes were examined using a light microscope (Eclipse E800, Nikon, Tokyo, Japan).

BAL and cell differentials in BAL fluid

BAL was performed as described previously [13,14], and the total number of cells in the BAL fluid was counted with a hemocytometer. For differential counts of leukocytes in BAL fluid, cytospin smear slides (Lab Systems; Tokyo, Japan) were prepared and stained with Diff-Quick Romanowski stain (Muto Kagaku Co., Tokyo, Japan).
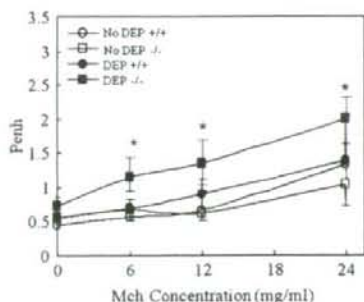
Figure 1   Airway hyperresponsiveness was assessed by whole-body plethysmography with free-moving application and then evaluated by Penh values in response to inhaled aerosolized methacholine (0, 6, 12, 24 mg/ml). The X axis shows the concentration of methacholine (mg/ml); the Y axis shows the values of Penh. $^{+/+}$, wild-type mice; $^{-/-}$, Nrf2 knockout mice. Results are means±SD of data in each group ($n=16$). *$p < 0.05$ Nrf2$^{-/-}$ mice vs Nrf2$^{+/+}$ mice at each methacholine concentration point.

Measurement of cytokines/chemokines in BAL fluid

Immunoreactivity for IL-12, IL-4, IL-13, MCP-1, eotaxin, RANTES, and TARC in the BAL fluid supernatants was measured with an enzyme-linked immunosorbent assay (ELISA) kit (Biosource International, Inc., Camarillo, CA). ELISA was carried out in accordance with the manufacturer's instruction sheet. Each sample was assayed in triplicate.

Measurement of IgG$_1$, IgG$_{2a}$, and IgE in serum

Immunoreactivity for IgG$_1$, IgG$_{2a}$ (Cygnus Technologies, Inc., Southport, NC), and IgE (Bethyl Laboratories, Inc., Montgomery, TX) in the serum was measured with an ELISA kit in accordance with the manufacturer's instruction sheet. Each sample was assayed in triplicate.

Quantitative real-time reverse transcription-polymerase chain reaction (RT-PCR)

Total RNA was extracted from the lung tissues with TRIzol Reagent (Gibco BRL, Gaithersburg, MD) in accordance with the manufacturer's instructions. Complementary DNA (cDNA) was synthesized as described previously [25] and quantified with a sequence detector (7900HT Sequence Detection System; Applied Biosystems) using PCR Master Mix and the respective inventoried primers including a β-actin control (TaqMan Universal PCR Master Mix, Applied Biosystems). TaqMan assays were repeated in triplicate samples for each of the selected antioxidant enzyme genes in each lung sample. The mRNA expression levels for all samples were normalized to the level of the housekeeping gene β-actin. Selected antioxidant enzyme genes and their assay ID were as follows: glutamate-cysteine ligase, modifier subunit (GCLm, Mm00514996_m1), glutamate-cysteine ligase, catalytic subunit (GCLc, Mm00802655_m1), glucose-6-phosphate dehydrogenase X-linked (G6PD, Mm00656735_g1), glutathione-S-transferase, alpha3 (GST-α3, Mm00494798_m1),

glutathione-S-transferase m1 (GST-M1, Mm00833915_g1), glutathione-S-transferase pi2 (GST-P2, Mm00839138_g1), heme-oxygenase-1 (HO-1, Mm00516004_m1), superoxide dismutase 2 (SOD2, Mm00449726_m1), glutathione reductase 1 (GSr, Mm00833903_m1), and β-actin (Mm00607939_s1).

Statistical analysis

Results are shown as means±standard deviation (SD). Differences between groups were determined by Student's t test using the Stat Mate III software package (ATMS Digitals Medical Station, Tokyo, Japan). Differences at $p < 0.05$ were considered significant.

Results

Assessment of changes in AHR in response to DEP exposure

To examine airway responses to low-dose DEP in Nrf2$^{-/-}$ mice, we first assessed AHR (as expressed in Penh) using whole-body plethysmography.

Exposure to DEP significantly increased the airway reactivity to methacholine (6, 12, and 24 mg/ml) in Nrf2$^{-/-}$ mice compared with Nrf2$^{+/+}$ mice (Fig. 1).

Lung histopathology

The histological specimens revealed no change in response to DEP exposure in Nrf2$^{+/+}$ mice (Fig. 2), but PAS staining-positive mucus cell hyperplasia was evident in Nrf2$^{-/-}$ mice (Fig. 2B). There were no inflammatory cell infiltrates in either Nrf2$^{+/+}$ or Nrf2$^{-/-}$ mice.

BAL cell differentials

Examination of the BAL fluid showed that the total number of cells and the number of macrophages were significantly lower in Nrf2$^{-/-}$ mice than in Nrf2$^{+/+}$ mice. The numbers of lymphocytes and eosinophils in the BAL fluid after DEP exposure were significantly higher in Nrf2$^{-/-}$ mice than in Nrf2$^{+/+}$ mice (Fig. 3).

Cytokine/chemokine levels in BAL fluid

The levels of IL-12 and IL-13 in BAL fluid after DEP exposure were significantly higher in Nrf2$^{-/-}$ mice. The level of IL-4 in BAL fluid did not change significantly after DEP exposure in either Nrf2$^{+/+}$ or Nrf2$^{-/-}$ mice (Fig. 4A). The level of TARC in BAL fluid after DEP exposure was significantly greater in Nrf2$^{-/-}$ mice than in Nrf2$^{+/+}$ mice. The levels of monocyte chemoattractant protein (MCP)-1, regulated upon activation, normal T expressed and secreted (RANTES) and Eotaxin in tBAL fluid were not changed significantly after DEP exposure in either Nrf2$^{+/+}$ or Nrf2$^{-/-}$ mice (Fig. 4B).

IgG$_1$, IgG$_{2a}$, and IgE levels in serum

There were no significant changes in the levels of IgE, IgG$_1$ and IgG$_{2a}$ in serum after DEP exposure in either Nrf2$^{+/+}$ or Nrf2$^{-/-}$ mice (Fig. 5).
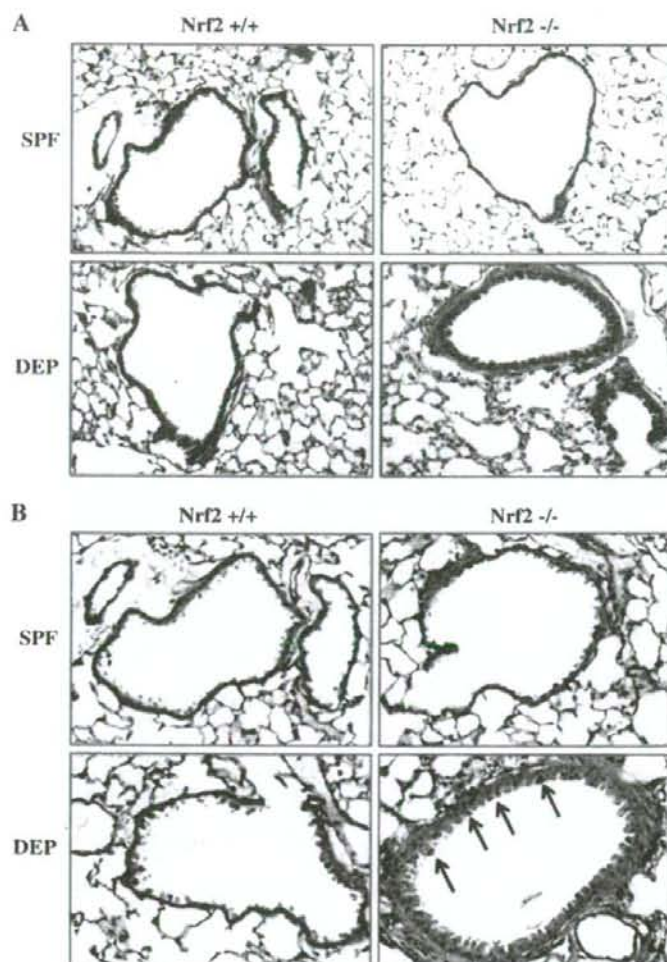
Figure 2 Histopathology of the lung tissues. Lung sections stained with HE and examined by light microscopy (100×) (A). Lung sections stained with PAS and examined by light microscopy (200×) (B). The arrows indicate the PAS-positive cells.
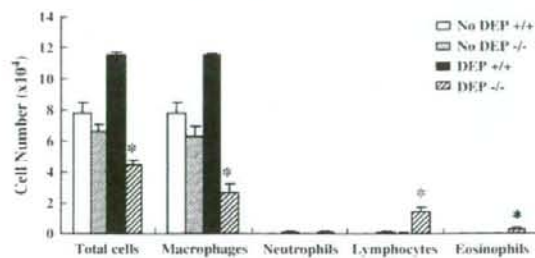

Figure 3 Changes in total cells and differentials in BAL fluid. The smear preparations in BAL fluid were stained with Diff-Quick Romanowski stain. Results are means ± SD of data in each group ($n=6$). *$p<0.05$ Nrf2$^{-/-}$ mice vs Nrf2$^{+/+}$ mice.
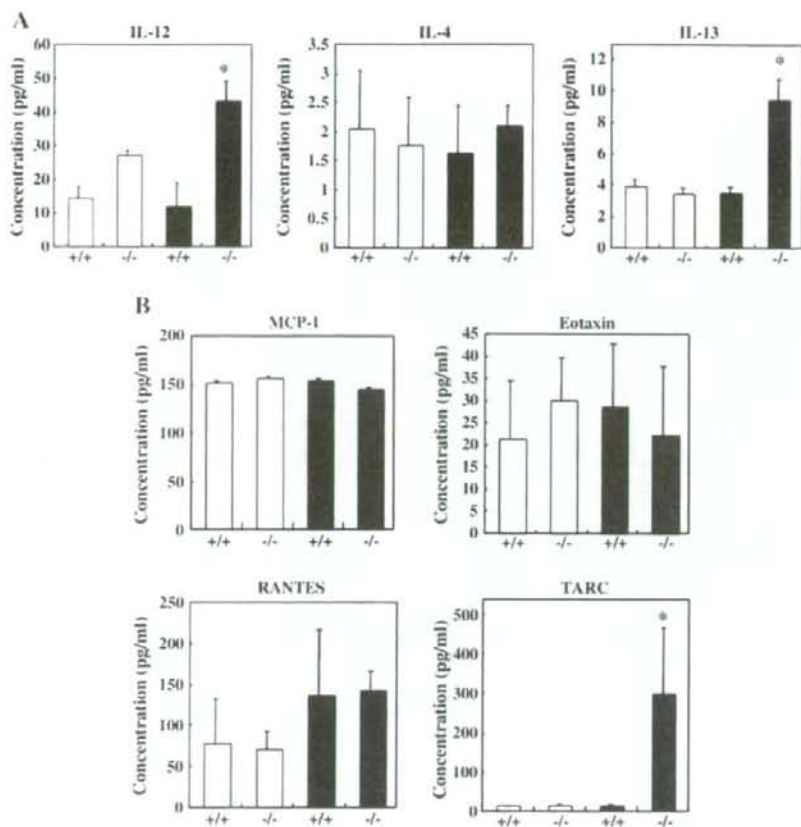
Figure 4 Cytokine (A) and chemokine (B) levels in BAL fluid as evaluated by ELISA. Clear bar, no DEP (not exposed to DEP) group; solid bar, DEP group; $^{+/+}$, wild-type mice; $^{-/-}$, Nrf2 knockout mice. Results are means ±SD of data in each group (n=6). *p<0.05 Nrf2$^{-/-}$ mice vs Nrf2$^{-/+}$ mice.

Induction of antioxidant enzyme genes in lung tissues

Changes in the expression of mRNA for various antioxidant enzymes were determined by real RT-PCR. After DEP exposure, the respective fold changes in mRNA expression in the lungs of Nrf2$^{+/+}$ and Nrf2$^{-/-}$ mice were: GCLm (3.4 vs 1.8), GCLc (5.5 vs 2.1), G6PD (18 vs 7.8), GST-α3 (7.4 vs 1.6), GST-M1 (6.2 vs 1.3), GST-P2 (6.4 vs 2.1), HO-1 (11.8 vs 6.9), SOD2 (17 vs 9.1), and GSr (8.8 vs 5.9) (Fig. 6). Thus, gene

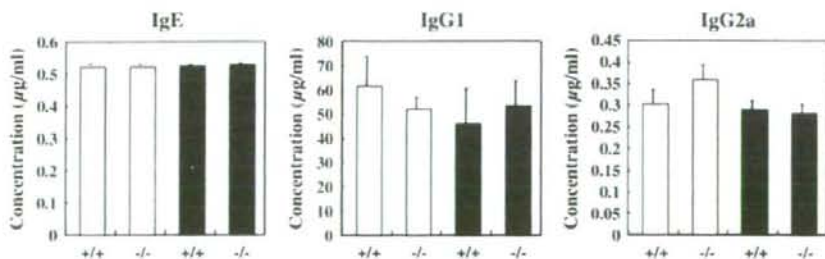
Figure 5 Immunoglobulin levels in sera evaluated by ELISA. Clear bar, no DEP (not exposed to DEP) group; solid bar, DEP group; $^{+/+}$, wild-type mice; $^{-/-}$, Nrf2 knockout mice. Results are means ±SD of data in each group (n=6).
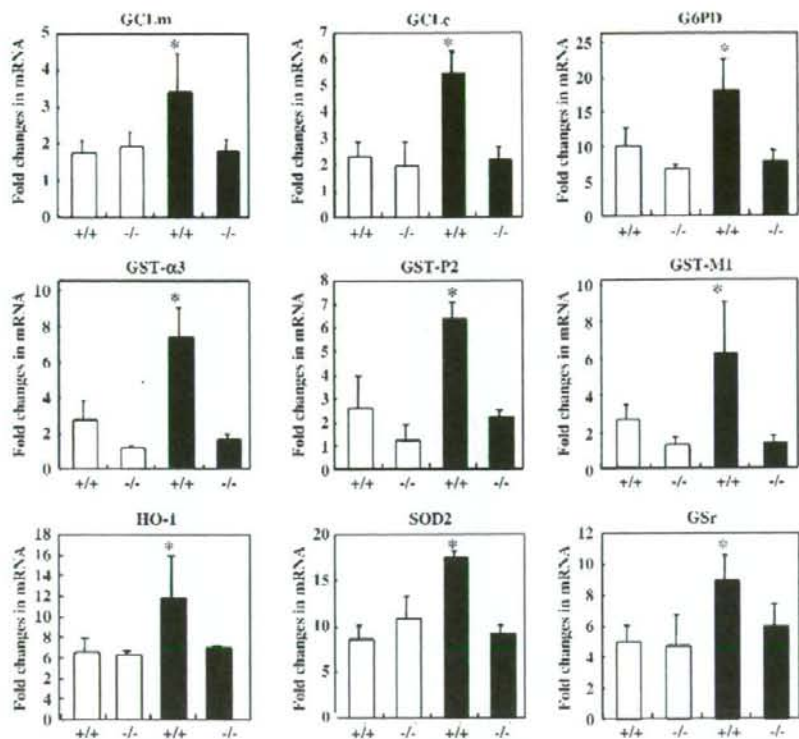
Figure 6   Real-time RT-PCR for genes of various antioxidants in the lungs. Clear bar, no DEP (not exposed to DEP) group; solid bar, DEP group; $^{+/+}$, wild-type mice; $^{-/-}$, Nrf2 knockout mice. Results are means ± SD of data in each group ($n=3$). $^*p<0.05$ Nrf2$^{-/-}$ mice vs Nrf2$^{+/+}$ mice.

expression of various antioxidant enzymes was significantly increased in Nrf2$^{+/+}$ mice compared with Nrf2$^{-/-}$ mice.

Discussion

The present study using Nrf2 gene knockout mice revealed for the first time that disruption of the Nrf2 gene enhanced susceptibility to airway inflammatory responses induced by inhalation of low-dose DEP. Nrf2$^{-/-}$ and Nrf2$^{+/+}$ C57BL/6 mice were exposed to low-dose DEP (i.e., at concentrations similar to those inhaled outdoors) for 8 weeks, and in Nrf2$^{-/-}$ mice significant increases of AHR, numbers of lymphocytes and eosinophils, and levels of IL-12, IL-13 and TARC in BAL fluid were observed in comparison with those of Nrf2$^{+/+}$ mice. In contrast, gene expression of antioxidant enzymes was significantly increased in Nrf2$^{+/+}$ mice in comparison with Nrf2$^{-/-}$ mice. As the magnitude of gene induction of these antioxidant enzymes was considerably higher in Nrf2$^{+/+}$ than in Nrf2$^{-/-}$ mice, it was clearly associated with the activation of Nrf2 in response to DEP-induced lung inflammation.

We assessed airway hyperresponsiveness (as expressed by enhanced Pause values (Penh)) by whole-body plethysmo-graphy. Penh has been used in an experimental mouse model to evaluate airway hyperresponsiveness [26–28]. Exposure to DEP increased airway reactivity to methacholine more significantly in Nrf2$^{-/-}$ mice than in Nrf2$^{+/+}$ mice. Our previous study showed that the changes in Penh induced by methacholine were significantly greater 1 week after DEP exposure in C57BL/6 mice, but that Penh recovered to the baseline level by 8 weeks after DEP exposure, and the changes in AHR were independent of the airway inflammation caused by oxidative stress derived from low-dose DEP exposure [13]. The current data suggest that AHR may increase with oxidative stress induced by continuous, long-term (longer than 8 weeks) exposure to DEP in wild-type mice. PAS-positive mucus cell hyperplasia was found only in Nrf2$^{-/-}$ mice, without destruction of the airway epithelial cells in the lung tissues. Although it has been confirmed that AHR increases with oxidative stress induced by DEP exposure, the mechanism by which AHR increases in Nrf2$^{-/-}$ mice is still unclear. It is speculated that, in this system, the changes in AHR caused by low-dose DEP may depend on the genetic strain of mouse employed, as reported by Depuydt et al. [29]. Our results suggest that Nrf2 plays a key role in regulation of AHR in oxidative stress caused by DEP exposure.

The total numbers of cells and macrophages in BAL fluid were significantly decreased, and the numbers of lymphocytes and eosinophils were significantly greater, after DEP exposure in Nrf2$^{-/-}$ mice than in Nrf2$^{+/+}$ mice. It is interesting that the changes in these differential cell counts in C57BL/6 Nrf2$^{-/-}$ mice 8 weeks after DEP exposure were similar to those previously reported in C57BL/6 wild-type mice 6 months after DEP exposure [14]. IL-12 influences the cytokine profile after T-cell activation [30]. Eosinophil recruitment into inflammatory sites is a complex process regulated by a number of cytokines including IL-13 [31]. Our findings suggest that IL-13 may be involved in eosinophil recruitment into the airways of Nrf2$^{-/-}$ mice after DEP exposure, possibly indicating the presence of novel lymphocyte-directed chemokines [32,33]. We found that the level of TARC, but not that of eotaxin or RANTES, was significantly increased. Dias-Sanchez et al. have suggested that the effects of DEP on cytokine/chemokine expression are not global or non-specific [34]. Among these CC chemokines, TARC was the first one shown to selectively chemoattract T lymphocytes [32]. TARC was subsequently identified by induction of T-cell chemotaxis, especially in Th2-type CD4$^+$ T lymphocytes [33]. TARC is a pivotal chemokine for the development of Th2-dominated experimental asthma with eosinophilia and AHR [35]. Our present results indicate that TARC is also an important chemokine in the development of Th2-dominated oxidative stress-induced airway inflammation after DEP exposure.

Although it is reported that the effects of DEP-induced oxidative stress initiate and exacerbate airway allergic responses through enhanced IgE production [36,37], in the low-dose DEP exposure systems, no remarkable changes in IgE were evident in serum of Nrf2$^{-/-}$ mice after DEP exposure.

In response to DEP exposure in the present study, there was increased induction of antioxidant enzyme mRNA in the lungs of Nrf2$^{+/+}$ mice. γ GCLm and GCLc are involved in glutathione (GSH) synthesis. GSH is the major intracellular thiol antioxidant that acts directly as a ROS scavenger. The GSH redox system plays a critical role in determining intracellular redox balance and antioxidant function [38]. GSR uses quinine oxidoreductase 1 (NADPH) for regeneration of reduced glutathione. G6PD, the enzyme involved in NADPH regeneration, was also considerably induced in Nrf2$^{+/+}$ mice in response to DEP. Our data clearly show that Nrf2 regulates several antioxidant enzyme genes that block oxidative stress and inflammation induced by DEP. The mRNA expression of other Nrf2-regulated antioxidant enzymes including GST-α3, GST-p2, GST-M1, SOD2 and HO-1 also increased in the Nrf2$^{+/+}$ mice. Our data indicate that Nrf2 deficiency results in reduced gene expression of antioxidant enzymes that block oxidative injury, leading to enhancement of inflammatory cell activity and AHR.

It has been reported that the pathogenesis of allergic asthma is related to oxidative stress [16]. In conjunction with allergens, DEP act as an adjuvant to enhance allergic responses such as expression of cytokines/chemokines and increased AHR [12,39]. It is conceivable that DEP exaggerate allergic asthmatic responses, and that the responses result from oxidative stress induced by DEP exposure.

In this study we showed for the first time that disruption of the Nrf2 gene facilitated susceptibility to airway inflammatory responses induced by inhalation of low-dose DEP in mice. These results strongly suggest that DEP-induced oxidative stress and host antioxidant responses play a key role in the development of DEP-induced airway inflammation, and may contribute to exaggeration of lung diseases related to oxidative stress such as allergic asthma.

Acknowledgment

References

[1] D.W. Dockery, C.A. Pope, X. Xu, J.D. Spengler, J.H. Ware, M.E. Fay, B.G. Ferris, F.E. Speizer, An association between air pollution and mortality in six U.S. cities, N. Engl. J. Med. 329 (1993) 1753–1759.

[2] J.M. Samet, F. Dominici, F.C. Curriero, I. Coursac, S.L. Zeger, Fine particulate air pollution and mortality in 20 U.S. cities, 1987–1994, N. Engl. J. Med. 343 (2000) 1742–1749.

[3] G. Hoek, B. Brunekreef, S. Goldbohm, P. Fischer, P.A. van den Brandt, Association between mortality and indicators of traffic-related air pollution in the Netherlands: a cohort study, Lancet 360 (2002) 1203–1209.

[4] A. Saxon, D. Diaz-Sanchez, Air pollution and allergy: you are what you breathe, Nat. Immunol. 6 (2005) 223–226.

[5] D. Diaz-Sanchez, L. Proietti, R. Polosa, Diesel fumes and the rising prevalence of atopy: an urban legend? Curr. Allergy Asthma Rep. 3 (2003) 146–152.

[6] H. Takizawa, T. Ohtoshi, S. Kawasaki, T. Kohyama, M. Desaki, T. Kasama, K. Kobayashi, K. Nakahara, K. Yamamoto, K. Matsushima, S. Kudoh, Diesel exhaust particles induce NF-kappa B activation in human bronchial epithelial cells in vitro: importance in cytokine transcription, J. Immunol. 162 (1999) 4705–4711.

[7] H. Takizawa, S. Abe, H. Okazaki, T. Kohyama, I. Sugawara, Y. Saito, T. Ohtoshi, S. Kawasaki, M. Desaki, K. Nakahara, K. Yamamoto, K. Matsushima, M. Tanaka, M. Sagai, S. Kudoh, Diesel exhaust particles upregulate eotaxin gene expression in human bronchial epithelial cells via nuclear factor-kappa B-dependent pathway, Am. J. Physiol. Lung. Cell Mol. Physiol. 284 (2003) L1055–1062.

[8] S. Hashimoto, Y. Gon, I. Takeshita, K. Matsumoto, I. Jibiki, H. Takizawa, S. Kudoh, T. Horie, Diesel exhaust particles activate p38 MAP kinase to produce interleukin 8 and RANTES by human bronchial epithelial cells and N-acetylcysteine attenuates p38 MAP kinase activation, Am. J. Respir. Crit. Care Med. 161 (2000) 280–285.

[9] G.G. Xiao, M. Wang, N. Li, J.A. Loo, A.E. Nel, Use of proteomics to demonstrate a hierarchical oxidative stress response to diesel exhaust particle chemicals in a macrophage cell line, J. Biol. Chem. 278 (2003) 50781–50790.

[10] N. Li, M.I. Venkatesan, A. Miguel, R. Kaplan, C. Gujuluva, J. Alam, A. Nel, Induction of heme oxygenase-1 expression in macrophages by diesel exhaust particle chemicals and quinones via the antioxidant-responsive element, J. Immunol. 165 (2000) 3393–3401.

[11] N. Li, J. Alam, M.I. Venkatesan, A. Eiguren-Fernandez, D. Schmitz, E. Di Stefano, N. Slaughter, E. Killeen, X. Wang, A. Huang, M. Wang, A.H. Miguel, A. Cho, C. Sioutas, A.E. Nel, Nrf2 is a key transcription factor that regulates antioxidant defense in macrophages and epithelial cells: protecting against the proinflammatory and oxidizing effects of diesel exhaust chemicals, J. Immunol. 173 (2004) 3467–3481.

[12] A. Matsumoto, K. Hiramatsu, Y.J. Li, A. Azuma, S. Kudoh, H. Takizawa, I. Sugawara, Repeated exposure to low-dose diesel

exhaust after allergen challenge exaggerates asthmatic responses in mice, Clin. Immunol. 121 (2006) 227–235.

[13] Y.J. Li, T. Kawada, A. Matsumoto, A. Azuma, S. Kudoh, H. Takizawa, I. Sugawara, Airway inflammatory responses to oxidative stress induced by low-dose diesel exhaust particle exposure differ between mouse strains, Exp. Lung Res. 33 (2007) 227–244.

[14] Y.J. Li, T. Kawada, H. Takizawa, A. Azuma, S. Kudoh, I. Sugawara, Y. Yamauchi, T. Kohyama, Airway inflammatory responses to oxidative stress induced by prolonged low-dose diesel exhaust particle exposure from birth differ between mouse BALB/c and C57BL/6 strains, Exp. Lung Res. 34 (2008) 125–139.

[15] T. Nguyen, P.J. Sherratt, C.B. Pickett, Regulatory mechanisms controlling gene expression mediated by the antioxidant response element, Annu. Rev. Pharmacol. Toxicol. 43 (2003) 233–260.

[16] T. Rangasamy, J. Guo, W.A. Mitzner, J. Roman, A. Singh, A.D. Fryer, M. Yamamoto, T.W. Kensler, R.M. Tuder, S.N. Georas, S. Biswal, Disruption of Nrf2 enhances susceptibility to severe airway inflammation and asthma in mice, J. Exp. Med. 202 (2005) 47–59.

[17] H.Y. Cho, S.P. Reddy, M. Yamamoto, S.R. Kleeberger, The transcription factor NRF2 protects against pulmonary fibrosis, FASEB J. 18 (2004) 1258–1260.

[18] T. Iizuka, Y. Ishii, K. Itoh, T. Kiwamoto, T. Kimura, Y. Matsuno, Y. Morishima, A.E. Hegab, S. Homma, A. Nomura, T. Sakamoto, M. Shimura, A. Yoshida, M. Yamamoto, K. Sekizawa, Nrf2-deficient mice are highly susceptible to cigarette smoke-induced emphysema, Genes Cells 10 (2005) 1113–1125.

[19] Y. Aoki, H. Sato, N. Nishimura, S. Takahashi, K. Itoh, M. Yamamoto, Accelerated DNA adduct formation in the lung of the Nrf2 knockout mouse exposed to diesel exhaust, Toxicol. Appl. Pharmacol. 173 (2001) 154–160.

[20] K. Itoh, T. Chiba, S. Takahashi, T. Ishii, K. Igarashi, Y. Katoh, T. Oyake, N. Hayashi, K. Satoh, I. Hatayama, M. Yamamoto, Y. Nabeshima, An Nrf2/small Maf heterodimer mediates the induction of phase II detoxifying enzyme genes through antioxidant response elements, Biochem. Biophys. Res. Commun. 236 (1997) 313–322.

[21] M. Ramos-Gomez, M.K. Kwak, P.M. Dolan, K. Itoh, M. Yamamoto, P. Talalay, T.W. Kensler, Sensitivity to carcinogenesis is increased and chemoprotective efficacy of enzyme inducers is lost in nrf2 transcription factor-deficient mice, Proc. Natl. Acad. Sci. U. S. A. 98 (2001) 2941–2943.

[22] Y. Saito, A. Azuma, S. Kudoh, H. Takizawa, I. Sugawara, Long-term inhalation of diesel exhaust affects cytokine expression in murine lung tissues: comparison between low- and high-dose diesel exhaust exposure, Exp. Lung Res. 28 (2002) 493–506.

[23] K. Hiramatsu, A. Azuma, S. Kudoh, M. Desaki, H. Takizawa, I. Sugawara, Inhalation of diesel exhaust for three months affects major cytokine expression and induces bronchus-associated lymphoid tissue formation in murine lungs, Exp. Lung Res. 29 (2003) 607–622.

[24] E. Hamelmann, J. Schwarze, K. Takeda, A. Oshiba, G.L. Larsen, C.G. Irvin, E.W. Gelfand, Noninvasive measurement of airway responsiveness in allergic mice using barometric plethysmography, Am. J. Respir. Crit. Care Med. 156 (1997) 766–775.

[25] S. Abe, H. Takizawa, I. Sugawara, S. Kudoh, Diesel exhaust (DE)-induced cytokine expression in human bronchial epithelial

cells: a study with a new cell exposure system to freshly generated DE in vitro, Am. J. Respir. Cell Mol. Biol. 22 (2000) 296–303.

[26] S.A. Shore, I.N. Schwartzman, B. Le Blanc, G.G. Murthy, C.M. Doerschuk, Tumor necrosis factor receptor 2 contributes to ozone-induced airway hyperresponsiveness in mice, Am. J. Respir. Crit. Care Med. 164 (2001) 602–607.

[27] S. Finotto, G.T. De Sanctis, H.A. Lehr, U. Herz, M. Buerke, M. Schipp, B. Bartsch, R. Atreya, E. Schmitt, P.R. Galle, H. Renz, M.F. Neurath, Treatment of allergic airway inflammation and hyperresponsiveness by antisense-induced local blockade of GATA-3 expression, J. Exp. Med. 193 (2001) 1247–1260.

[28] A.S. Leme, C. Hubeau, Y. Xiang, A. Goldman, K. Hamada, Y. Suzaki, L. Kobzik, Role of breast milk in a mouse model of maternal transmission of asthma susceptibility, J. Immunol. 165 (2006) 762–769.

[29] P. Depuydt, G.F. Joos, R.A. Pauwels, Ambient ozone concentrations induce airway hyperresponsiveness in some rat strains, Eur. Respir. J. 38 (1999) 14125–14131.

[30] S.L. Prescott, A. Taylor, B. King, J. Dunstan, J.W. Upham, C.A. Thornton, P.G. Holt, Neonatal interleukin-12 capacity is associated with variations in allergen-specific immune responses in the neonatal and postnatal periods, Clin. Exp. Allergy 33 (2003) 566–572.

[31] M.E. Rothenberg, Eosinophilia, N. Engl. J. Med. 338 (1998) 1592–1600.

[32] T. Imai, M. Baba, M. Nishimura, M. Kakizaki, S. Takagi, O. Yoshie, The T cell-directed CC chemokine TARC is a highly specific biological ligand for CC chemokine receptor 4, J. Biol. Chem. 272 (1997) 15036–15042.

[33] T. Imai, D. Chantry, C.J. Raport, C.L. Wood, M. Nishimura, R. Godiska, O. Yoshie, P.W. Gray, Macrophage-derived chemokine is a functional ligand for the CC chemokine receptor 4, J. Biol. Chem. 273 (1997) 1764–1768.

[34] D. Diaz-Sanchez, M. Jyrala, D. Ng, A. Nel, A. Saxon, In vivo nasal challenge with diesel exhaust particles enhances expression of the CC chemokines rantes, MIP-1alpha, and MCP-3 in humans, Clin. Immunol. 97 (2000) 140–145.

[35] S. Kawasaki, H. Takizawa, H. Yoneyama, T. Nakayama, R. Fujisawa, M. Izumizaki, T. Imai, O. Yoshie, I. Homma, K. Yamamoto, K. Matsushima, Intervention of thymus and activation-regulated chemokine attenuates the development of allergic airway inflammation and hyperresponsiveness in mice, J. Immunol. 166 (2001) 2055–2062.

[36] M.J. Whitekus, N. Li, M. Zhang, M. Wang, M.A. Horwitz, S.K. Nelson, L.D. Horwitz, N. Brechun, D. Diaz-Sanchez, A.E. Nel, Thiol antioxidants inhibit the adjuvant effects of aerosolized diesel exhaust particles in a murine model for. ovalbumin sensitization, J. Immunol. 168 (2002) 2560–2567.

[37] J. Wan, D. Diaz-Sanchez, Phase II enzymes induction blocks the enhanced IgE production in B cells by diesel exhaust particles, J. Immunol. 177 (2006) 3477–3483.

[38] A. Meister, Glutathione deficiency produced by inhibition of its synthesis, and its reversal; applications in research and therapy, Pharmacol. Ther. 51 (1991) 155–194.

[39] Y. Miyabara, H. Takano, T. Ichinose, H.B. Lim, M. Sagai, Diesel exhaust enhances allergic airway inflammation and hyperresponsiveness in mice, Am. J. Respir. Crit. Care Med. 157 (1998) 1138–1144.

Aire controls the differentiation program of thymic epithelial cells in the medulla for the establishment of self-tolerance

Masashi Yano,[1] Noriyuki Kuroda,[1] Hongwei Han,[1]
Makiko Meguro-Horike,[1] Yumiko Nishikawa,[1] Hiroshi Kiyonari,[2]
Kentaro Maemura,[3] Yuchio Yanagawa,[4] Kunihiko Obata,[5]
Satoru Takahashi,[6] Tomokatsu Ikawa,[7] Rumi Satoh,[7] Hiroshi Kawamoto,[7]
Yasuhiro Mouri,[1] and Mitsuru Matsumoto[1]

[1]Division of Molecular Immunology, Institute for Enzyme Research, University of Tokushima, Tokushima 770-8503, Japan
[2]Laboratory for Animal Resources and Genetic Engineering, Center for Developmental Biology, Institute of Physical and Chemical Research (RIKEN) Kobe, Kobe 650-0047, Japan
[3]Department of Anatomy and Cell Biology, Division of Basic Medicine I, Osaka Medical College, Osaka, 569-8686, Japan
[4]Department of Genetic and Behavioral Neuroscience, Gunma University Graduate School of Medicine, Maebashi 371-8511, Japan
[5]Neuronal Circuit Mechanisms Research Group, RIKEN Brain Science Institute, Saitama 351-0198, Japan
[6]Institute of Basic Medical Sciences and Laboratory Animal Resource Center, Center for Tsukuba Advanced Research Alliance, University of Tsukuba, Tsukuba 305-8575, Japan
[7]Laboratory for Lymphocyte Development, RIKEN Research Center for Allergy and Immunology, Kanagawa 230-0045, Japan

The roles of autoimmune regulator (Aire) in the expression of the diverse arrays of tissue-restricted antigen (TRA) genes from thymic epithelial cells in the medulla (medullary thymic epithelial cells [mTECs]) and in organization of the thymic microenvironment are enigmatic. We approached this issue by creating a mouse strain in which the coding sequence of green fluorescent protein (GFP) was inserted into the *Aire* locus in a manner allowing concomitant disruption of functional Aire protein expression. We found that Aire+ (i.e., GFP+) mTECs were the major cell types responsible for the expression of Aire-dependent TRA genes such as *insulin 2* and *salivary protein 1*, whereas Aire-independent TRA genes such as *C-reactive protein* and *glutamate decarboxylase 67* were expressed from both Aire+ and Aire− mTECs. Remarkably, absence of Aire from mTECs caused morphological changes together with altered distribution of mTECs committed to Aire expression. Furthermore, we found that the numbers of mTECs that express involucrin, a marker for terminal epidermal differentiation, were reduced in Aire-deficient mouse thymus, which was associated with nearly an absence of Hassall's corpuscle-like structures in the medulla. Our results suggest that Aire controls the differentiation program of mTECs, thereby organizing the global mTEC integrity that enables TRA expression from terminally differentiated mTECs in the thymic microenvironment.

CORRESPONDENCE
Mitsuru Matsumoto:
mitsuru@ier.tokushima-u.ac.jp

Abbreviations used: Ab, antibody; Ag, antigen; Aire, autoimmune regulator; APECED, autoimmune-polyendocrinopathy-candidiasis ectodermal dystrophy; CRP, C-reactive protein; EpCAM, epithelial cell adhesion molecule 1; FSC, forward scatter; GAD67, glutamate decarboxylase 67; K5, keratin 5; mTEC, medullary thymic epithelial cell; SAP1, salivary protein 1; SSC, side scatter; TRA, tissue-restricted Ag; UEA-1, *Ulex europaeus* agglutinin 1.

Autoimmune diseases are mediated by sustained adaptive immune responses specific for self-antigens (Ags) through unknown pathogenic mechanisms. Although breakdown of self-tolerance is considered to be the key event in the disease process, the mechanisms that allow the production of autoantibodies and/or autoreactive lymphocytes are largely enigmatic (1). Autoimmune-polyendocrinopathy-candidiasis ectodermal dystrophy (APECED; OMIM 240300)

is a rather rare autoimmune disease affecting mainly the endocrine glands. Because mutation of a single gene, *autoimmune regulator (AIRE)*, is solely responsible for the development of APECED, understanding the relationship between *AIRE* gene malfunction and the breakdown of self-tolerance promises to help unravel

The online version of this article contains supplemental material.

2827

the pathogenesis of not only APECED but also other types of autoimmune diseases (2, 3).

One of the most important aspects of AIRE in the context of autoimmunity is its limited tissue expression in medullary thymic epithelial cells (mTEC) (4, 5). mTECs are believed to play major roles in the establishment of self-tolerance by eliminating autoreactive T cells (negative selection) and/or by producing immunoregulatory T cells, which together prevent CD4^{+} T cell–mediated organ-specific autoimmune diseases (6, 7). For this purpose, mTECs appear to express a set of self-Ags encompassing many or most of the self-Ags expressed by parenchymal organs. Supporting this hypothesis, analysis of gene expression in the thymic stroma has demonstrated that mTECs are a specialized cell type in which promiscuous expression of a broad range of peripheral tissue-restricted Ag (TRA) genes (i.e., promiscuous gene expression) is an autonomous property (8). Aire in mTECs has been suggested to regulate this promiscuous gene expression (9–11) through as yet undetermined mechanisms.

From a mechanistic viewpoint, there are two possible models to explain the function of Aire in the thymic organogenesis required for the establishment of self-tolerance. First, Aire may play a tolerogenic role within the types of mTECs characterized by Aire expression. In other words, the presence of Aire within cells is necessary in order for them to function normally as tolerance-establishing cells. Consistent with this idea, the current prevailing view on the roles of Aire in establishing self-tolerance is that Aire-positive cells are the major cell types that show promiscuous gene expression and that the lack of Aire protein within cells impairs their tolerogenic function because of the reduced transcription of TRA genes, although the developmental process of mTECs is otherwise unaltered in the absence of Aire (model 1). The second model hypothesizes that Aire is necessary for the developmental program of mTECs, including Aire-positive cells themselves. In this case, we assume that what are called Aire-positive mTECs and other Aire-dependent cell-types do not develop normally in the absence of Aire. Given that acquisition of the properties of promiscuous gene expression depends on the maturation status of mTECs (see Results and Discussion), impaired promiscuous gene expression from Aire-deficient mice can be associated with a defect of such an Aire-dependent developmental program in mTECs (model 2). Although it is still controversial whether reduced transcription of particular TRA genes in Aire-deficient mTECs can account for the development of autoimmunity targeting the corresponding self-Ags in Aire-deficient mice by itself (11–15), it is critical to determine which model provides a more appropriate explanation of Aire-dependent promiscuous gene expression to further elucidate the molecular aspects of Aire (16). Model 1 would direct research toward the mechanisms underlying how a single *Aire* gene can regulate a large number of target genes (i.e., TRA genes), whereas model 2 would accelerate studies of the developmental program of mTECs in which Aire plays a pivotal role. These two models can be tested if we can monitor the developmental process of mTECs committed to Aire expression in both the presence and absence of functional Aire protein.

This issue regarding the roles of Aire in thymic organogenesis is also directly linked to the fundamental question of how mTECs acquire their unique ability to express a broad range of self-Ags (i.e., promiscuous gene expression). The terminal differentiation model assumes that mTECs eventually acquire the capacity for promiscuous gene expression by becoming differentiated, more mature, and more promiscuous (7, 10). This model suggests that mTECs, especially Aire-positive cells, are specialized cell types that have acquired this ability through differentiation. In this context, it is noteworthy that the transcriptional machinery necessary for promiscuous gene expression other than Aire protein is considered to be acquired by mTECs independent of Aire expression in this model. The model suggests that the transcriptional unit for promiscuous gene expression becomes fully active when Aire starts to be expressed in terminally differentiated mTECs. In contrast, the developmental model considers that promiscuous gene expression is a reflection of the multipotency of immature mTECs before the developmental fate of particular cell types is determined (17). In this model, expression of a broad spectrum of TRA genes is regulated by conserved developmental programs that are active in developing mTECs, and Aire and/or Aire^{+} cells control this process (18). Accordingly, the developmental model considers that Aire acts at the early developmental stage of mTEC differentiation, which is in marked contrast to the timing of Aire expression proposed in the terminal differentiation model. Thus, the terminal differentiation model and the developmental model favor models 1 and 2, respectively, proposed for the roles of Aire in promiscuous gene expression and self-tolerance (19).

To investigate in more detail the roles of Aire in thymic organogenesis, we have used a knock-in mouse strategy in which the coding sequence of GFP was inserted into the *Aire* gene locus in a manner allowing concomitant disruption of functional Aire protein expression. This strategy allowed us to distinguish mTECs committed to expressing Aire from Aire-nonexpressing mTECs, in both the presence and absence of functional Aire protein. In addition, with the use of knock-in mice in which thymic TRA (i.e., *glutamate decarboxylase 67* [*GAD67*]) expression can be monitored by GFP expression we also examined the cell types of mTECs responsible for promiscuous gene expression in situ. The results suggest that Aire promotes the differentiation program of mTECs and that promiscuous gene expression is accomplished in terminally differentiated mTECs that have fully matured in the presence of Aire protein.

RESULTS

Establishment of Aire/GFP knock-in mice

To examine the molecular and cellular contribution of Aire to thymic organogenesis, we established Aire/GFP knock-in mice in which expression of the GFP gene is under the transcriptional control of the endogenous *Aire* gene. In this strategy, modification of the *Aire* gene locus was minimized by inserting a GFP-neomycin resistance (neo[r]) gene cassette (gfp-neo) (20) between exon 1 and exon 2 (Fig. 1 A). After

establishing $Aire^{+/gfp-neo}$ mice, they were crossed with a general deleter Cre recombinase-expressing transgenic line (21) to remove the neo' gene cassette, which contains the herpes simplex virus *thymidine kinase* gene promoter for efficient neo' gene expression. After confirming the removal of the neo' gene cassette (Fig. 1 B), mice were crossed with C57BL/6 mice to select a line containing the GFP knock-in allele but not the Cre recombinase-expressing transgenic allele. $Aire^{+/gfp}$ mice were then crossed to obtain $Aire^{gfp/gfp}$ mice, which have a null mutation for the *Aire* gene because of disruption of the *Aire* gene by insertion of the GFP gene (Fig. 1 B). As expected, $Aire^{gfp/gfp}$ mice, but not $Aire^{+/gfp}$ mice, showed no expression of endogenous Aire in the thymus, as detected with polyclonal anti–Aire antibody (Ab) recognizing peptides located within the proline-rich region of Aire (unpublished data).

Using immunohistochemistry, we first examined whether GFP expression from $Aire^{+/gfp}$ mouse thymus reflects endogenous *Aire* gene expression. Stromal cells showing variable extents of GFP expression in the cytoplasm and nucleus were scattered throughout the thymic medulla (Fig. 1 C). The medullary region was identified by staining with *Ulex europaeus* agglutinin 1 (UEA-1) (Fig. 2 A), anti–epithelial cell adhesion molecule 1 (EpCAM) mAb (Fig. 2 B), or anti–keratin 5 (K5) Ab (Fig. S1 A, available at http://www.jem.org/cgi/content/full/jem.20080046/DC1). GFP-expressing cells from $Aire^{+/gfp}$ mouse thymus showed a dendritic to fibroblastic morphology and were enriched at the cortico-medullary junction (Fig. 1 C; Fig. 2, A and B; and Fig. S1 A). When doubly stained with anti–Aire Ab, most of the GFP-expressing cells contained variable amounts of Aire nuclear dots within their nuclei (Fig. 1 C), indicating that GFP expression is under the

transcriptional control of the authentic *Aire* gene. However, a few cells showed Aire nuclear dots without any detectable GFP expression (Fig. 1 C, arrows) or expressed GFP without obvious Aire nuclear dots (not depicted). As expected, $Aire^{+/+}$ mouse thymus showed no GFP signals (Fig. 2, A and B). Notably, most of the CD11c-positive DCs in the thymus were GFP negative (Fig. S1 B), suggesting that Aire expression from thymic DCs is negligible compared with that from mTECs.

Altered thymic organization in Aire-deficient mice

We then examined the effect of Aire deficiency on thymic organization in $Aire^{gfp/gfp}$ mouse thymus sections, focusing on the production of cells genetically marked with GFP and, therefore, active in *Aire* gene transcription but lacking functional Aire protein. There were many GFP⁺ "Aire-less" TECs within the medulla (Figs. 2, A and B; and Fig. S1 A), indicating clearly that Aire protein itself is not necessary for the production of particular mTEC lineages committed to express Aire. However, detailed inspection demonstrated that the morphology and location of GFP⁺ cells from $Aire^{gfp/gfp}$ thymus were altered compared with those of GFP⁺ cells containing functional Aire protein from $Aire^{+/gfp}$ mouse thymus. First, we noticed that the cell shape of GFP⁺ mTECs lacking functional Aire protein was altered; in $Aire^{gfp/gfp}$ thymus, more GFP⁺ cells exhibited a globular shape instead of a dendritic to fibroblastic morphology, compared with $Aire^{+/gfp}$ thymus (Fig. 2 C, arrows). The lower preponderance of a dendritic shape of GFP⁺ Aire-less mTECs was verified by statistical analysis. We calculated the level of cell shape complexity for each GFP⁺ cell by dividing the length of the cellular periphery by the cell area using a computer program (i.e., the higher
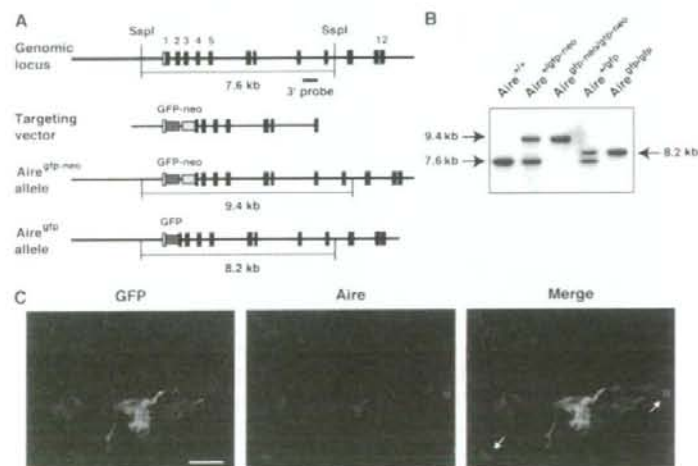

Figure 1. **Establishment of Aire/GFP knock-in mice.** (A) Targeted insertion of the GFP gene into the *Aire* gene locus by homologous recombination. SspI, *SspI* restriction site. (B) Southern blot analysis of genomic DNA from offspring of Aire/GFP knock-in mice. Tail DNA was digested with *SspI* and hybridized with the 3' probe shown in A. (C) Concomitant expression of GFP (green) and endogenous mouse Aire (red) assessed by immunohistochemistry of a thymus section from an $Aire^{+/gfp}$ mouse. Cells positive for Aire staining but negative for GFP expression are marked with arrows. Bar, 20 µm. One representative experiment from a total of four repeats is shown.

the value, the more complex the cell shape). GFP$^+$ cells from *Aire$^{gfp/gfp}$* thymus showed lower values (i.e., less complexity per cell) and a narrower distribution of values (i.e., less heterogeneity of cell shape) than those from *Aire$^{+/gfp}$* thymus (Fig. 2 D). Because a gene-dosage effect has been noticed at the *Aire* gene locus (11), we carefully excluded the possibility that the altered shape of GFP$^+$ cells from *Aire$^{gfp/gfp}$* thymus was due simply to higher GFP protein expression within each cell, i.e., imposing a potentially toxic burden on the cells. For this purpose, we crossed *Aire$^{+/gfp}$* mice with *Aire$^{-/-}$* mice (12) to establish *Aire$^{-/gfp}$* mice in which the *gfp* allele is single, as in *Aire$^{+/gfp}$* mice (Fig. S2 A). Similarly to the *Aire$^{gfp/gfp}$* thymus analysis, GFP$^+$ cells from *Aire$^{-/gfp}$* thymus demonstrated less complexity of cell shape than those from *Aire$^{+/gfp}$* thymus, as confirmed using the same method of statistical analysis (Fig. S2 B).

Although we analyzed the thymic organization of *Aire$^{gfp/gfp}$* mice before the onset of autoimmune pathology (i.e., 4–6 wk after birth), we also excluded the possibility that the altered cell shape of GFP$^+$ cells from *Aire$^{gfp/gfp}$* thymus was secondary to the autoimmune phenotypes by establishing *Aire$^{-/gfp}$* mice expressing the OT-II TCR transgene in which the autoreactive T cell repertoire is absent (Fig. S3 A). Morphological changes in GFP$^+$ cells were similarly observed in these mice (Fig. S3 B), suggesting that the altered shape of GFP$^+$ cells lacking Aire protein was independent of autoimmune phenotype.

Second, we noticed that the distribution pattern of mTECs committed to Aire expression was also affected in the absence of functional Aire protein. In contrast with the enrichment of GFP$^+$ cells from *Aire$^{+/gfp}$* thymus at the cortico-medullary junction, GFP$^+$ cells from *Aire$^{gfp/gfp}$* thymus tended to be localized
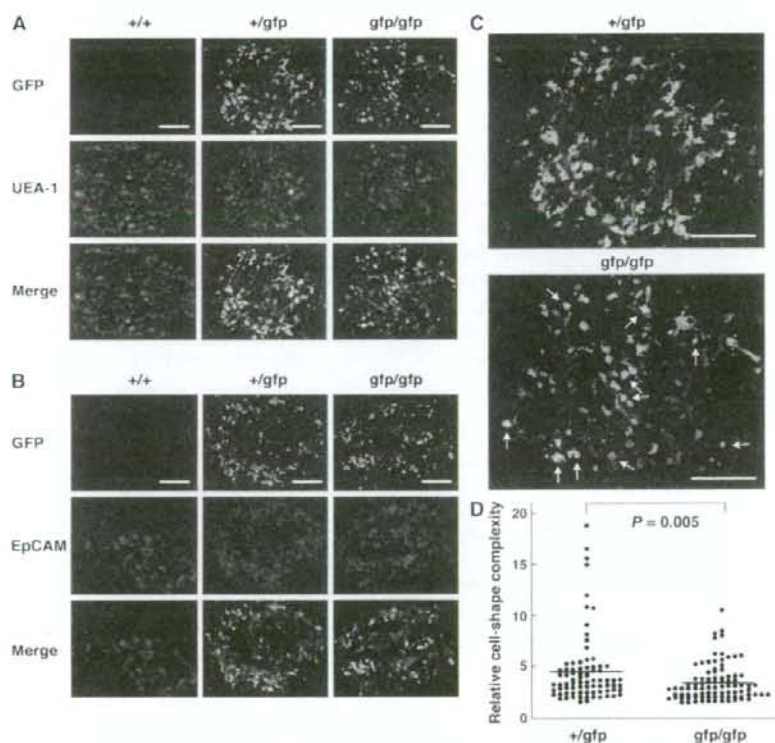
Figure 2. Altered morphology and distribution of mTECs committed to express Aire in the absence of functional Aire protein.
(A and B) mTECs active in *Aire* gene transcription were visualized by immunohistochemistry with anti-GFP Ab (green). The medullary region was identified by staining with UEA-1 (A) or anti-EpCAM mAb (B; red). Bars, 100 μm. One representative experiment from a total of five repeats is shown. (C) Enlargement of the staining with anti-GFP Ab from A for demonstration of altered morphology and distribution of mTECs committed to express Aire in *Aire$^{gfp/gfp}$* mouse thymus. There were more GFP$^+$ cells with globular shapes (bottom, arrows) in *Aire$^{gfp/gfp}$* thymus than in *Aire$^{+/gfp}$* thymus. GFP$^+$ cells from *Aire$^{+/gfp}$* thymus were enriched at the cortico-medullary junction (top), whereas GFP$^+$ cells from *Aire$^{gfp/gfp}$* thymus tended to be localized more evenly within each medulla or even enriched at the center of the medulla (bottom). Bars, 100 μm. One representative experiment from a total of five repeats is shown. (D) Morphological changes in the shape of GFP$^+$ cells from *Aire$^{gfp/gfp}$* mouse thymus demonstrated in C were analyzed statistically. Each circle corresponds to the relative cell shape complexity of a single GFP$^+$ cell calculated with a computer program (see Materials and methods). A total of 80 and 88 GFP$^+$ cells from *Aire$^{+/gfp}$* and *Aire$^{gfp/gfp}$* thymi, respectively, were evaluated. Red lines represent mean values. Two mice for each group were analyzed, and similar results were obtained from a total of three repeats.

more uniformly within each medulla or even enriched at the medulla center (Fig. 2 C and Fig. S1 A). Altered distribution of GFP⁺ Aire-less mTECs was also evident in *Aire⁻/ᵍᶠᵖ* mice (Fig. S2 A), as well as in *Aire⁻/ᵍᶠᵖ* mice expressing the nonautoreactive OT-II TCR transgene (Fig. S3 A). Collectively, production of a particular mTEC lineage committed to express Aire is not determined by Aire protein alone. However, Aire deficiency in these cells results in morphological changes together with altered location within the medulla, suggesting a role of Aire in the differentiation program of mTECs in a cell-intrinsic manner.

Analysis of embryonic thymus demonstrated that GFP⁺ cells were absent at embryonic day 13.5, but clearly present at embryonic day 16.5 in both *Aire⁺/ᵍᶠᵖ* and *Aireᵍᶠᵖ/ᵍᶠᵖ* mice (Fig. S1 C). Although the effect of absence of Aire protein on the location of GFP⁺ cells from *Aireᵍᶠᵖ/ᵍᶠᵖ* mice at the embryonic and early P1 (postneonatal) stages was difficult to evaluate because of the less organized thymic structure together with relatively small numbers of GFP⁺ cells at those stages, morphological alteration of each mTEC committed to Aire expression was already evident at the neonatal stage (P1; Fig. S4 A), as confirmed by the same statistical analysis applied to Fig. 2 D (Fig. S4 B). The properties of GFP⁻ (i.e., Aire nonexpressing) mTECs as evaluated by immunohistochemistry with UEA-1, anti-EpCAM Ab (Fig. 2, A and B), anti-K5 Ab (Fig. S1 A), ER-TR5 Ab, anti-claudin 3/4 Abs, and MTS10 Ab (not depicted) showed no obvious difference between *Aire⁺/ᵍᶠᵖ* and *Aireᵍᶠᵖ/ᵍᶠᵖ* adult thymi.

In addition to the histological evaluation of mTECs based on Aire/GFP expression, another possibility that Aire controls the differentiation program of mTECs has emerged from studies focusing on the cell differentiation markers expressed by mTECs. In the skin, involucrin expression is restricted to postmitotic epithelial cells and serves as a marker of epidermal and follicular terminal differentiation (22). Interestingly, immunohistochemistry of the human thymus using anti-involucrin Ab stains characteristic swirled epithelial structures known as Hassall's corpuscles (23), which is consistent with the fact that Hassall's corpuscles are composed of terminally differentiated mTECs (24). When thymus sections from Aire-sufficient mice were stained with anti-involucrin Ab, involucrin-expressing cells were scattered within the EpCAM⁺ thymic medulla (Fig. 3 A). The number of involucrin-expressing cells was age dependent and declined between 8 and 11 wk (Fig. 3 B and Table S1, available at http://www.jem.org/cgi/content/full/jem.20080046/DC1). In addition, we occasionally found larger involucrin-expressing structures with a hyalinized degenerated core in the thymic medulla from Aire-sufficient mice, which is reminiscent of Hassall's corpuscles in human thymus (Fig. 3 C). Remarkably, the numbers of mTECs expressing involucrin in Aire-deficient mice were significantly lower than those in Aire-sufficient mice, especially at 4 and 8 wk of age (Fig. 3 B). Furthermore, we observed no typical Hassall's corpuscle-like structures in the thymus of Aire-deficient mice at any age, which is in contrast to those seen in Aire-sufficient mice (Table S1). These results further support

the notion that lack of Aire in mTECs alters their differentiation program, thereby altering mTEC integrity.

Next, we used flow cytometric analysis to examine GFP-expressing cells from the thymus. Thymic stromal cells were released enzymatically from adult thymi and stained with anti-CD45 mAb and UEA-1, together with anti-CD80 and anti–MHC class II mAbs. *Aire⁺/ᵍᶠᵖ* thymus contained 4.5% UEA-1⁺GFP⁺ (i.e., Aire⁺) cells (from here on simply designated GFP⁺ cells) in the population of CD45⁻ stromal cells (Fig. 4 A). When forward scatter (FSC) and side scatter (SSC) parameters were compared between GFP⁺ cells and UEA-1⁺GFP⁻ cells (from here on simply designated GFP⁻ cells), GFP⁺ cells were larger and more broadly distributed compared with GFP⁻ cells (Fig. 4 B, left), suggesting a distinct cellular morphology of Aire⁺ cells among mTECs. *Aireᵍᶠᵖ/ᵍᶠᵖ* thymus also contained GFP⁺ cells in the population of CD45⁻ stromal cells (Fig. 4 A), as already observed by immunohistochemical analysis (Figs. 2 and S1). Interestingly, the proportion of GFP⁺ cells in *Aireᵍᶠᵖ/ᵍᶠᵖ* thymus was consistently
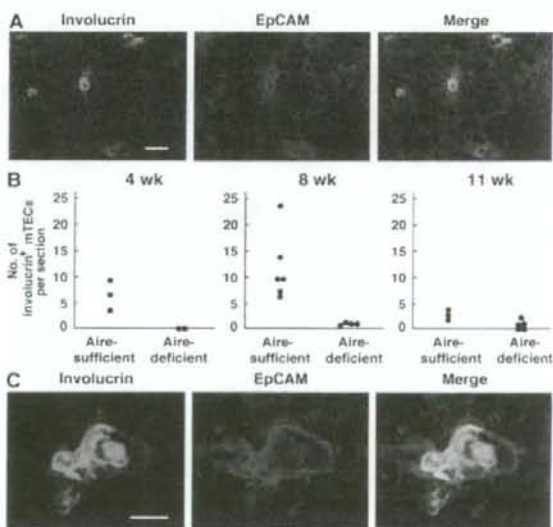
Figure 3. **Reduced numbers of terminally differentiated mTECs in the absence of Aire.** (A) Involucrin-expressing mTECs (green) were scattered within the thymic medulla (red; stained with anti-EpCAM Ab) of Aire-sufficient mice. Bar, 50 μm. (B) Numbers of involucrin-expressing mTECs were reduced in Aire-deficient mice at 4 (left) and 8 (middle) wk of age. Numbers of involucrin-expressing mTECs in Aire-sufficient mice declined at 11 wk of age (right). Each circle corresponds to the mean number of involucrin-expressing mTECs per section examined in individual mice. Detailed information for the mice examined from a total of five experiments is presented in Table S1 (available at http://www.jem.org/cgi/content/full/jem.20080046/DC1). (C) Hassall's corpuscle-like structures seen in Aire-sufficient mouse thymus stained with anti-involucrin Ab (green) together with anti-EpCAM Ab (red). These discrete and larger involucrin-expressing structures were scarcely detectable in Aire-deficient mouse thymus. Bar, 20 μm. One representative experiment from a total of five repeats is shown.

30–40% higher than in *Aire*[+/gfp] thymus (Fig. 4 A). Consequently, the ratio of GFP^{+} cells to GFP^{−} cells was higher in *Aire*[gfp/gfp] thymus (~1:5) compared with that in *Aire*[+/gfp] thymus (~1:10). Although the difference in FSC/SSC parameters between GFP[+] and GFP^{−} cells observed for *Aire*[+/gfp] mice was also seen in *Aire*[gfp/gfp] mice (Fig. 4 B, right), FSC/SSC plots of GFP^{+} cells from *Aire*[gfp/gfp] mice showed a more condensed profile over a narrower region compared with GFP^{+} cells from *Aire*[+/gfp] mice (Fig. 4 B, top), which might reflect the morphological changes in GFP^{+} mTECs observed by immunohistochemistry (Fig. 2 C). We recorded no GFP expression from CD45^{+} hematopoietic cells (not depicted) or from CD45^{−}UEA-1^{−} thymic stromal cells from either *Aire*[+/gfp] or *Aire*[gfp/gfp] mice (Fig. 4 A).

We then analyzed the expression of CD80 and MHC class II from each of the populations separated on the basis of GFP expression and UEA-1 binding. GFP^{+} cells from *Aire*[+/gfp] mice expressed both CD80 and MHC class II at high levels (CD80^{hi}/class II^{hi}), whereas GFP^{−} cells from the same animals expressed intermediate to low levels of both CD80 and MHC class II (Fig. 4 C, left). GFP^{+} cells from *Aire*[gfp/gfp] thymus were also CD80^{hi}/class II^{hi} (Fig. 4 C, right), indicating that expression of these Ag presentation-related molecules was Aire independent. Indeed, expression levels of both CD80 and

MHC class II from GFP^{+} cells were almost indistinguishable between *Aire*[+/gfp] and *Aire*[gfp/gfp] mice when the two flow cytometric profiles were merged (Fig. 4 D, left). However, although difference was small, expression of both CD80 and MHC class II from GFP^{−} cells from *Aire*[gfp/gfp] mice was consistently lower than that from *Aire*[+/gfp] mice (Fig. 4 D, right). This result may indicate that the absence of normal Aire-expressing cells from the medulla is accompanied by phenotypic alteration of Aire-nonexpressing mTECs, which was not evident with the immunohistochemical analysis with the commonly used medullary epithelial cell markers (Fig. 2, A and B; and Fig. S1 A). Collectively, the results suggest that Aire deficiency results in a global alteration of the thymic microenvironment that involves not only mTECs committed to express Aire but also the Aire-nonexpressing mTECs that surround Aire^{+} cells.

Aire-dependent TRA gene expression

Although Aire has been suggested to regulate promiscuous gene expression in mTECs (9, 10), demonstration that Aire^{+} cells are the major source of promiscuous gene expression from mTECs is still incomplete in the absence of appropriate cell markers for Aire-expressing cell lineages. Existing data for promiscuous gene expression from mTECs were obtained
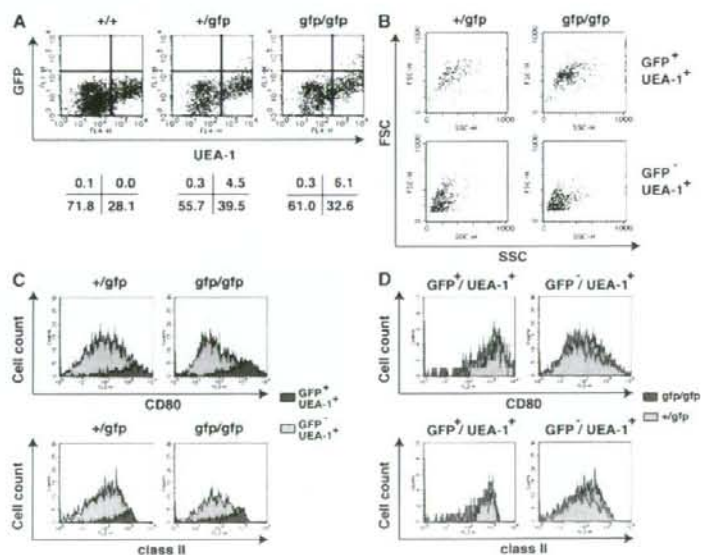
Figure 4. Global alteration of mTEC phenotypes in the absence of Aire. (A) Detection of GFP-expressing cells from thymic stroma by flow cytometric analysis. CD45^{−} thymic stromal cells were analyzed for the expression of GFP together with binding of UEA-1. Percentages of cells from each fraction are indicated below. (B) mTECs committed to express Aire were larger than mTECs noncommitted to express Aire, irrespective of the presence of Aire protein. FSC/SSC profiles of mTECs committed to express Aire were altered in the absence of functional Aire protein (top). Each FSC/SSC profile was obtained by back gating the corresponding fractions from A based on the expression of GFP and UEA-1. (C) CD80 and MHC class II expression levels were higher in mTECs committed to express Aire than in mTECs noncommitted to express Aire, irrespective of the presence of functional Aire protein. Filled profiles in green and gray are from GFP[+] and GFP[−] mTECs, respectively. (D) CD80 and MHC class II expression from mTECs committed to express Aire were indistinguishable between *Aire*[+/gfp] and *Aire*[gfp/gfp] mice (left) but were reduced in mTECs noncommitted to express Aire in the absence of functional Aire protein (right). Filled profiles in gray and green lines are from *Aire*[+/gfp] and *Aire*[gfp/gfp] mice, respectively. Flow cytometric profiles from C were merged for comparison. One representative result from a total of more than five repeats is shown.

by flow cytometric sorting using surrogate Aire[+] cell markers such as CD80 and MHC class II. As a result, it is not yet clear which population of mTECs (i.e., Aire-expressing or Aire-nonexpressing mTECs) is deficient in promiscuous gene expression as a result of absence of functional Aire protein. To answer this question, we separated GFP[+] and GFP[−] mTECs from both *Aire[+/dh]* and *Aire[dh/dh]* mice and examined the expression of several TRA genes, including both Aire-dependent (i.e., *insulin 2* and *salivary protein 1 [SAP1]*) and Aire-independent (*C-reactive protein [CRP]*) TRA genes; expression of the former and the latter gene classes has been demonstrated to be reduced or unchanged, respectively, in CD80^{hi}/class II^{hi} Aire-deficient mTECs (9, 10). GFP^{+} mTECs from *Aire[+/dh]* mice showed the highest expression of *insulin 2* and *SAP1*, and expression of those genes was much lower in GFP[−] mTECs from the same animals (Fig. 5). Remarkably, both GFP[+] and GFP[−] mTECs from *Aire[dh/dh]* mice expressed almost none of the Aire-dependent TRA genes *insulin 2* and *SAP1*. mTECs defined by UEA-1 binding from *Aire^{+/+}* mice, which includes both Aire[+] and Aire^{−} cells, showed intermediate expression of those genes. These results clearly indicate two important features of promiscuous gene expression in mTECs. First, Aire[+] mTECs are the major cell types responsible for the expression of Aire-dependent TRA genes. Second, mTECs cannot express Aire-dependent TRA genes in the absence of functional Aire protein, even though the lineage commitment to express Aire and the expression of Ag presentation-related molecules, such as CD80 and MHC class II, are preserved (Fig. 4 C). It is important to emphasize that the latter observation does not necessarily mean that Aire acts on the already existing transcriptional machinery required for TRA gene expression within established terminally differentiated mTECs. Rather, in the light of the fact that GFP[+] Aire-less mTECs show defective

development, as indicated by their altered morphology and distribution, we suggest that Aire[+] mTECs acquire their unique machinery for promiscuous gene expression only when they have fully achieved maturation with the help of Aire protein (see Discussion and see Fig. 8).

In marked contrast to Aire-dependent TRA genes, expression of an Aire-independent TRA gene, *CRP*, from GFP[+] mTECs was indistinguishable between *Aire[+/dh]* and *Aire[dh/dh]* mice. *CRP* expression from GFP[−] mTECs was detectable, although the levels were lower than from GFP[+] mTECs, and was also similar between *Aire[+/dh]* and *Aire[dh/dh]* mice (Fig. 5). As expected, the *Aire* gene was highly expressed from GFP[+] mTECs of *Aire[+/dh]* mice, although a low level of *Aire* gene expression was detected from GFP[−] mTECs, which is possibly a result of slight contamination by cells expressing a trace amount of GFP (i.e., Aire) in this fraction. Expression of the *Aire* gene from both GFP[+] and GFP^{−} cells of *Aire[dh/dh]* mice was at background levels.

Aire-independent TRA gene expression in situ from mTECs

The results in the previous section suggest that individual mTECs do not express a broad array of TRA genes. Rather, each mTEC seems to express a different spectrum of TRA genes. Some TRA genes, such as *insulin 2* and *SAP1* (previously recognized as Aire-dependent genes; references 9, 10), were predominantly expressed from cells of the Aire[+] mTEC lineage only when Aire protein was present within the cells, and other TRA genes, such as *CRP* (previously recognized as an Aire-independent gene; references 9, 10), were expressed from both Aire[+] and Aire[−] mTECs irrespective of the presence of Aire protein. The latter situation was further investigated with the use of GAD67/GFP knock-in mice (*GAD67[+/dh]* mice). *GAD67*, an Aire-independent TRA gene that is expressed in the brain and pancreas, is
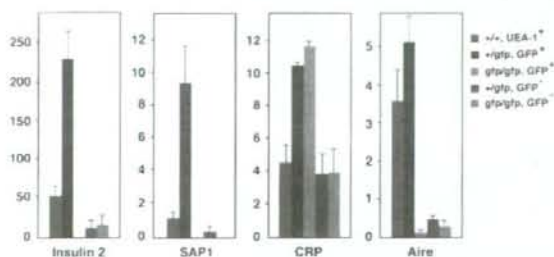
Figure 5. TRA gene expression from mTECs assessed by real-time PCR. Expression of *insulin 2*, *SAP1*, *CRP*, and *Aire* was examined from each fraction of mTECs sorted on the basis of the flow cytometric profile demonstrated in Fig. 4 A. Color bars corresponding to each fraction are indicated on the right. Aire[+] mTECs were the major cell types responsible for the expression of Aire-dependent TRA genes (*insulin 2* and *SAP1*), whereas an Aire-independent TRA gene (*CRP*) was expressed from both Aire[+] and Aire[−] mTEC fraction. Aire expression was assessed to verify the proper sorting of each mTEC fraction. Numbers are relative gene expression level compared with that of the *Hprt* gene. Results are expressed as the mean ± SEM for triplicate wells of one representative experiment from a total of three repeat experiments.
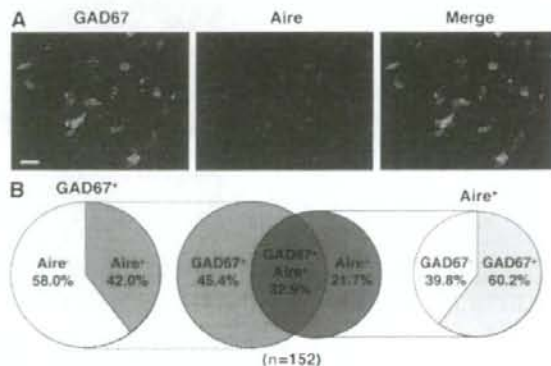
Figure 6. Expression of the Aire-independent TRA gene GAD67 and of Aire from mTECs in situ. (A) Expression of the *GAD67* gene and Aire was detected by immunohistochemistry with anti-GFP Ab (green) and anti-Aire Ab (red), respectively, in thymus sections from GAD67/GFP knock-in mice. Bar, 20 μm. (B) Results obtained as described for A were calculated for a total of 152 mTECs expressing the *GAD67* gene and/or Aire. One representative experiment from a total of three repeats is shown.

also active in mTECs from $GAD67^{+/gfp}$ mice (25). Using immunohistochemistry, we examined the expression of GAD67 together with Aire in $GAD67^{+/gfp}$ mouse thymus sections. There were three types of TECs: GAD67⁺Aire⁻ (45.4%), GAD67⁺Aire⁺ (32.9%), and GAD67⁻Aire⁺ (21.7%) (Fig. 6, A and B). Among the GAD67⁺ mTECs, 42.0% expressed Aire and the rest did not (Fig. 6 B), consistent with the Aire-independent nature of GAD67 gene expression (9, 10). Conversely, among the Aire⁺ mTECs, 60.2% expressed GAD67 and the rest did not, suggesting that Aire expression is not sufficient for TRA expression, at least for this Aire-independent TRA gene.

## Expression of *Aire* and Aire-independent TRA genes by nonproliferating mTECs

Previous studies suggested that Aire is predominantly expressed by terminally differentiated cells on the basis of their poor incorporation of BrdU (26, 27). We confirmed this finding by injecting BrdU into $Aire^{+/gfp}$ mice. BrdU incorporation was scarce in GFP⁺ mTECs (Fig. 7 A, top). We similarly examined which type of mTECs, immature proliferating or mature nonproliferating, express GAD67 by injecting BrdU into GAD67/GFP knock-in mice. We found that GFP⁺ mTECs incorporated BrdU only weakly (Fig. 7 A, bottom), suggesting that expression of this Aire-independent TRA gene

is also imposed on terminally differentiated cells rather on immature proliferating mTECs.

p63 is strongly expressed in epithelial stem cells of the thymus and specifically functions to maintain their extraordinary proliferative capacity (28). To examine whether mTECs expressing the *Aire* and *GAD67* genes have this high proliferative capacity, we examined p63 expression from thymi of Aire/GFP knock-in and GAD67/GFP knock-in adult mice. mTECs expressing GFP from both mouse strains showed little p63 expression by immunohistochemistry (Fig. 7 B), suggesting that neither of these genes is expressed in mTECs with high proliferative capacity. Instead, Aire seems to function within mTECs in the later stages of differentiation, when the cells are also responsible for TRA gene expression.

DISCUSSION

In the present study, we addressed fundamental questions regarding how mTECs acquire the capacity for promiscuous gene expression with the participation of Aire, with the hope that understanding the roles of Aire in thymic organogenesis will help to unravel the molecular mechanisms responsible for expression of immunological self in the thymic microenvironment. The issues include the following: first, whether Aire itself is necessary for the production and/or differentiation
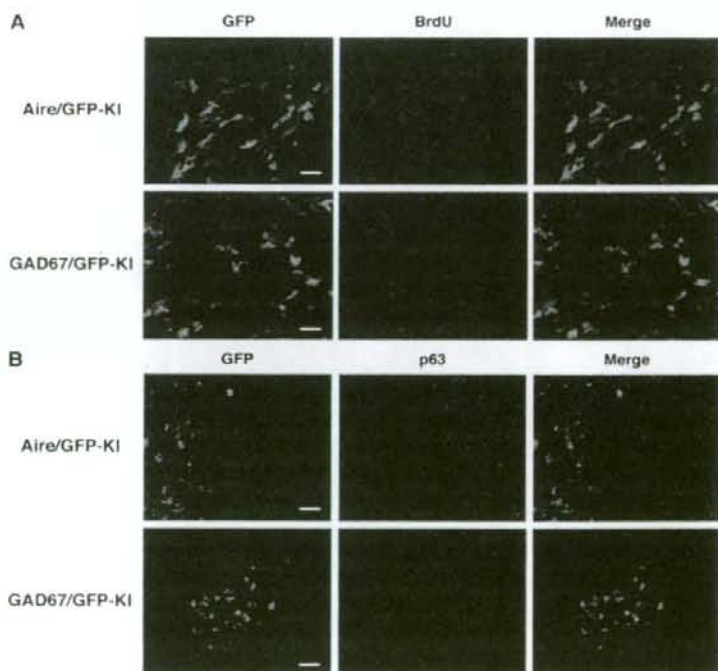
Figure 7. Expression of the *Aire* and *GAD67* genes by nonproliferating mTECs. (A) BrdU incorporation by *Aire-* and *GAD67*-expressing mTECs was evaluated 4 h after i.p. injection of BrdU into $Aire^{+/gfp}$ and $GAD67^{+/gfp}$ mice, respectively. The thymus sections were stained with anti-GFP (green) and anti-BrdU (red) Abs. Bars, 20 μm. (B) p63 (red) was not detected in mTECs expressing the *Aire* and *GAD67* genes (green). Bars, 40 μm. One representative experiment from a total of four repeats is shown.

program of Aire⁺ cell lineages; second, whether Aire⁺ mTECs are necessary for the structural and/or functional organization of other types of mTECs; third, to what extent Aire⁺ mTECs contribute to the expression of TRA genes; and fourth, the nature of the maturation status of mTECs that express Aire and are responsible for TRA expression. Because Aire-specific Ab cannot be used to investigate the differentiation process of mTECs committed to express Aire in the absence of Aire protein, we established Aire/GFP knock-in mice in which the GFP marker gene was inserted into the *Aire* gene locus in a manner allowing concomitant disruption of functional Aire protein expression. In *Aire⁺/ᵍᶠᵖ* mice, this strategy also enables us to distinguish Aire-expressing cells from Aire-nonexpressing cells without introducing any cell markers incompletely unique to Aire-expressing cells. Accordingly, mTECs committed to Aire expression were faithfully GFP marked with this strategy; mTECs transcriptionally active for the *Aire* gene were mostly positive for staining with anti-Aire Ab by immunohistochemistry. There were, however, small numbers of cells that were either positive for Aire staining but negative for *Aire* gene transcription (i.e., GFP⁻) or, conversely, positive for *Aire* gene transcription (i.e., GFP⁺) but negative for Aire staining. The former cell type could result from different half-lives of the two proteins (GFP vs. Aire), whereas the latter cell type could result from Aire protein being present as a diffuse nucleoplasmic form (more difficult to recognize) instead of the typical nuclear-dot form (29). Alternatively, these discrepancies could simply be accounted for by differences in detection sensitivity. Indeed, RT-PCR analysis of flow cytometry–sorted cell fractions showed the expected patterns of *Aire* gene expression.

With Aire/GFP knock-in mice, we have clearly demonstrated that Aire⁺ mTECs are the major cell types responsible for the expression of so-called Aire-dependent TRA genes such as *insulin 2* and *SAP1* (9, 10). These genes were almost exclusively expressed from GFP⁺ mTECs of *Aire⁺/ᵍᶠᵖ* mice but not of *Aireᵍᶠᵖ/ᵍᶠᵖ* mice. In contrast, expression of Aire-independent genes, such as *CRP*, was not affected by the absence of Aire. *CRP* expression from GFP⁺ cells was similar between *Aire⁺/ᵍᶠᵖ* and *Aireᵍᶠᵖ/ᵍᶠᵖ* mice. *CRP* expression, although at lower levels, was also observed from GFP⁻ cells and, again, was indistinguishable between *Aire⁺/ᵍᶠᵖ* and *Aireᵍᶠᵖ/ᵍᶠᵖ* mice. Expression of *GAD67* in an Aire-independent manner (9, 10) was also supported by immunohistochemistry of GAD67/GFP knock-in thymus, demonstrating *GAD67* expression irrespective of the presence of Aire protein in each mTEC. We speculate that the Aire dependency of TRAs reflects, in part, the cell types in which TRAs are expressed; expression of Aire-dependent genes is confined to Aire⁺ mTECs, whereas expression of Aire-independent genes occurs from both Aire⁺ and Aire⁻ mTECs. It is of note that mTECs do not uniformly express the overlapping spectrum of TRAs, as exemplified by the scattered expression of the *GAD67* gene in GAD67/GFP knock-in mouse thymus. Similarly, although Aire⁺ mTECs are the major cell types responsible for the expression of Aire-dependent TRA genes, this does not mean that all Aire⁺ mTECs
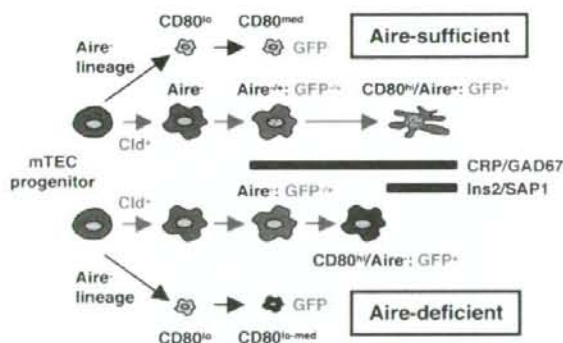
express Aire-dependent TRA genes uniformly. Indeed, single-cell analysis has demonstrated that expression of Aire in mTECs is not sufficient for simultaneous coexpression of Aire-dependent TRA genes (17). Thus, we favor the notion that promiscuous gene expression reflects the thymus-wide summation of expression of a small number of self-Ags by individual mTECs rather than expression of the complete spectrum of self-Ags by each cell (17, 18).

Because expression of transcription factors associated with developmental plasticity of progenitor cells (i.e., *Nanog, Oct4* and *Sox2*) is Aire-dependent in mTECs (18), the developmental model predicts that Aire acts early in the development of mTECs. The developmental model also suggests that promiscuous gene expression represents coordinated gene expression reflecting an alternate program of epithelial differentiation among actively proliferating mTECs at their progenitor or immature stages (19). However, accumulating data together with the results of the present study do not support such a view (26, 27). Rather, it is likely that Aire is acting at the late differentiation stages of mTECs. Accordingly, Aire-dependent processes for achieving promiscuous gene expression might also be active at the late differentiation stages of mTECs (see the subsequent paragraph). Clearly, this does not involve mTECs gaining the ability to express CD80 from CD80ˡᵒ precursors (30) because GFP⁺ mTECs from *Aireᵍᶠᵖ/ᵍᶠᵖ* mice demonstrated normal levels of CD80 expression. It is necessary to dissect the developmental process of mTECs, thereby precisely identifying the Aire-dependent steps of mTEC differentiation.

Given that Aire-expressing cells are terminally differentiated, the demonstration that Aire⁺ mTECs are the major cell types responsible for expression of TRA genes, at least for Aire-dependent genes, apparently favors the terminal differentiation model for Aire-dependent promiscuous gene expression from mTECs (7, 10, 11). However, our results do support a key aspect of a role for Aire in the developmental model (17–19): absence of Aire in mTECs causes morphological changes together with altered distribution of mTECs committed to express Aire. Indeed, the difference in appearance of GFP-expressing cells was distinct enough to allow discrimination between *Aire⁺/ᵍᶠᵖ* and *Aireᵍᶠᵖ/ᵍᶠᵖ* mouse sections by blind analysis. Interestingly, Gillard et al. (18) noted that globular mTECs without visible cellular projections were more prominent in Aire-deficient thymus, which could represent the GFP⁺ globular mTECs we observed in *Aireᵍᶠᵖ/ᵍᶠᵖ* mice. Furthermore, expression of functional molecules, such as CD80 and MHC class II from mTECs noncommitted to express Aire, was also affected by the absence of Aire, suggesting that Aire and/or Aire⁺ mTECs influence the organization of mTECs beyond simply controlling promiscuous gene expression within Aire-expressing cell lineages. We do not believe that the demonstration that terminally differentiated Aire-expressing cells are the major source of promiscuous gene expression (apparently favoring the terminal differentiation model) and the demonstration that Aire and/or Aire⁺ cells controls thymic organogenesis (consistent with the developmental model; reference 18 and present study) are mutually exclusive. Instead,

Aire could both promote the differentiation program of mTECs committed to express Aire, ensuring that they become fully equipped with the necessary machinery for promiscuous gene expression, and be an efficient driver of promiscuous gene expression in such cells. Thus, promiscuous gene expression seems to be accomplished in terminally differentiated mTECs that have matured in the presence of Aire protein (Fig. 8). Alternatively, Aire might be necessary for maintenance of a terminally differentiated state in which mTECs manifest a dendritic shape with fully competent promiscuous gene expression.

We found that the numbers of mTECs expressing involucrin, a marker of epidermal differentiation (22), were reduced in Aire-deficient mouse thymus. It was noteworthy that involucrin-expressing mTECs themselves were negative for Aire expression with immunohistochemistry (unpublished data), thus making it unlikely that *involucrin* gene expression in mTECs is under direct transcriptional control by Aire as a part of TRA gene expression. Similarly, it is unknown whether impaired involucrin expression is specific to mTECs committed to Aire expression or whether lack of Aire⁺ mTECs affects the differentiation of other type(s) of mTECs that would otherwise express involucrin at their terminally differentiated stages. Based on the fact that GFP⁺ Aire-less mTECs showed alterations in their morphology as well as distribution, we assume that the former possibility is more likely. Interestingly,

we found that reduction of involucrin-expressing mTECs in Aire-deficient mice was associated with a nearly absence of Hassall's corpuscle-like structures, although the exact relevance of this phenotype to the breakdown of central tolerance in Aire-deficient mice remains unknown (31). Together with the fact that formation of thymic cysts is a predominant feature of Aire-deficient mice (18, 26), it seems likely that Aire exerts more global control of the differentiation program of mTECs than was initially thought.

Finally, although we have demonstrated that Aire organizes the global mTEC integrity that facilitates promiscuous gene expression in the thymic microenvironment, the exact nature of the mTEC differentiation program under the control of Aire protein still remains unknown. We have demonstrated that both *Aire* and an Aire-independent TRA gene, *GAD67*, are predominantly expressed by nonproliferative cells, although we cannot completely exclude the possibility that expression of these genes is associated with immature cells that turn over slowly and, thus, would be poorly labeled by BrdU. The results prompt us to propose a fascinating hypothesis that promiscuous gene expression is achieved by induction of heterogeneity among terminally differentiated mTECs rather than by multipotentiality of mTEC progenitors. We speculate that Aire may contribute to mTEC heterogeneity by acting on mTECs at the late differentiation stages and that lack of Aire may result in failure to create this heterogeneity. According to this scenario, additional mechanisms for the development of Aire-dependent autoimmunity might be possible beyond reduced TRA expression from Aire-deficient mTECs, for instance, altered Ag processing and/or presentation capacity by Aire-deficient mTECs (12) and/or altered T cell development affecting establishment of the complete T cell repertoire. Study of the mechanisms underlying the Aire-dependent production of heterogeneity among mature mTECs might be a rewarding approach to elucidating the nature of the negative selection niche in the thymus.

Figure 8. Schematic representation of the roles of Aire in mTEC differentiation and TRA gene expression. Aire-expressing cell lineages develop from mTEC progenitor cells through concomitant expression of claudin (26). Expression of Aire-dependent TRA genes, such as *insulin 2* and *SAP1*, can be accomplished in terminally differentiated mTECs showing a dendritic to fibroblastic morphology that have fully matured with the help of Aire protein (marked as Aire-sufficient). Lack of Aire in mTECs results in premature termination of differentiation, although claudin⁺ Aire-expressing cell lineages can still develop and pass the CD80-expressing maturation stage (marked as Aire-deficient). These CD80ʰⁱ Aire-less mTECs have a more globular cell shape and lack transcriptional machinery for Aire-dependent TRA genes. Because Aire-independent TRA genes, such as *CRP* and *GAD67*, can be expressed before the terminal differentiation stages, lack of Aire has little impact on their expression. The possibility also remains that Aire is necessary for the maintenance of a terminally differentiated state, in which mTECs manifest a dendritic shape with fully competent promiscuous gene expression.

MATERIALS AND METHODS

Mice. Aire/GFP knock-in mice (RIKEN Center for Developmental Biology accession No. CDB0483K) were generated by gene targeting as described previously (32). In brief, the targeting vector was constructed by replacing the genomic *Aire* locus starting from exon 1 (immediately after the Kozak sequence) to exon 2 with a GFP-neomycin resistance (neoʳ) gene cassette (20). The neoʳ gene cassette harbors loxP sites at both ends. The targeting vector was introduced into TT2 embryonic stem cells (33), and the homologous recombinant clones were first identified by PCR and confirmed by Southern blot analysis. After the targeted cells had been injected into morula-stage embryos, the resulting chimeric male mice were mated with C57BL/6 females (CLEA) to establish germ-line transmission. *Aire*⁺/ᵍᶠᵖ⁻ⁿᵉᵒ mice were crossed with Ayu1-Cre mice (21), a general deleter Cre recombinase-expressing transgenic line, to remove the neoʳ gene cassette. After confirming removal of the neoʳ gene cassette, mice were crossed with C57BL/6 mice to select the line containing the GFP knock-in allele but not the Cre recombinase-expressing transgene. *Aire*⁺/ᵍᶠᵖ mice were then crossed to obtain *Aire*ᵍᶠᵖ/ᵍᶠᵖ mice, which have the null mutation for the *Aire* gene. GAD67/GFP knock-in mice were heterozygous for GAD67-GFP (Δneo) as described previously (34). OT-II transgenic mice (35) were purchased from The Jackson Laboratory. The mice were maintained under pathogen-free conditions.

The protocols used in this study were in accordance with the Guidelines for Animal Experimentation of Tokushima University School of Medicine and were conducted with the approval of the RIKEN Kobe Animal Experiment Committee.

Immunohistochemistry. Mice were killed and the thymus tissues were fixed as described previously (25, 36). Immunohistochemical analysis of the thymus with UEA-1 (Vector Laboratories), rat anti-EpCAM mAb (BD), and rabbit polyclonal anti-K5 Ab (Covance) was performed as described previously (37). Rabbit polyclonal anti-Aire Ab was produced as described previously (13). Goat polyclonal anti-GFP Ab (Novus Biologicals) and rabbit polyclonal anti-GFP Ab (Invitrogen) were used for the detection of GFP-expressing cells. BrdU incorporation by mTECs was examined 4 h after i.p. injection of 1 mg BrdU/mouse, and the detection of BrdU incorporation was performed with anti-BrdU Ab (BD), as described previously (26). Rabbit polyclonal anti-p63 Ab was purchased from Santa Cruz Biotechnology, Inc. The level of cell shape complexity for each GFP+ cell was calculated by dividing the length of the cellular periphery by the cell area (i.e., periphery/area × 1/4π) measured by the WinROOF program (Mitani Corporation). After obtaining photos of the thymus sections stained with anti-GFP Ab, the photos were subjected to analysis with the software. Immunohistochemistry of the thymus sections and statistical analysis of cell shape complexity from different genotype of mice for comparison were processed simultaneously in the same set of experiment to minimize variability between the assays. Numbers of involucrin-expressing mTECs were assessed after staining the thymus sections with rabbit polyclonal Ab against mouse involucrin (Covance). Well developed EpCAM+ thymic medullas were examined for the presence of involucrin-expressing cells from several thymus sections obtained from individual mice.

TEC preparation and flow cytometric analysis. TECs were prepared as described previously (12). In brief, thymic lobes were isolated from mice and cut into small pieces. The fragments were gently rotated in RPMI 1640 medium (Invitrogen) supplemented with 10% heat-inactivated FCS (Invitrogen), 20 mM Hepes, 100 U/ml penicillin, 100 µg/ml streptomycin, and 50 µM 2-ME at 4°C for 30 min and dispersed further with pipetting to remove the majority of thymocytes. The resulting thymic fragments were digested with 0.125% collagenase D (Roche) and 10 U/ml DNase I (Roche) in RPMI 1640 at 37°C for 15 min. The supernatants, containing dissociated TECs, were saved, and the remaining thymic fragments were further digested with collagenase D and DNase I. This step was repeated twice, and the remaining thymic fragments were digested with 0.125% collagenase/dispase (Roche) and DNase I at 37°C for 30 min. The supernatants from this digest were combined with the supernatants from the collagenase digests, and the mixture was centrifuged for 5 min at 450 g. The cells were suspended in PBS, containing 5 mM EDTA and 0.5% FCS, and kept on ice until the staining. The cells were stained with anti-CD45 mAb (BD) and UEA-1 and subjected to flow cytometric cell sorting with a FACS Vantage (BD). Flow cytometric analysis was performed after staining the cells with anti-CD45 mAb, UEA-1, anti-I-A^b (eBioscience), and anti-CD80 (eBioscience) mAbs with a FACSCalibur (BD) as described previously (13, 37).

Real-time PCR. RNA was extracted from sorted mTECs with RNeasy Mini kits (QIAGEN) and made into cDNA with cDNA Cycle kits (Invitrogen) according to the manufacturer's instructions. Real-time PCR for quantification of the *insulin 2, SAP1, CRP,* and *Hprt* genes was performed as described previously (12, 13). The primers and the probes are as follows: *insulin 2* primers, 5'-AGACCATCAGCAAGCAGGTC-3' and 5'-CTGGTG-CAGCACTGATCCAC-3'; *insulin 2* probe, 5'-FAM-CCCGGCAGAAG-CGTGGCATT-3'; *SAP1* primers, 5'-ACTCCTTGTGTTGCTTGGTG-TTT-3' and 5'-TCGACTGAATCAGAGGAATCAACT-3'; *SAP1* probe, 5'-FAM-TTCACCAGCAGAATCAGCAGTTCCAGAA-3'; *CRP* primers, 5'-TACTCTGGTGCCTTCTGATCATGA-3' and 5'-GGCTTCTTT-GACTCTGCTTCCA-3'; *CRP*probe,5'-FAM-CAGCTTCTCTCGGA-CTTTTGGTCATGA-3'; *Hprt* primers, 5'-TGAAGAGCTACTGTAAT-

GATCAGTCAAC-3' and 5'-AGCAAGCTTGCAACCTTAACCA-3'; and *Hprt* probe, 5'-FAM-TGCTTTCCCTGGTTAAGCAGTACAGCCC-3'.

Statistical analysis. All results are expressed as mean ± SEM. Statistical analysis was performed using Student's two-tailed unpaired t test for comparisons between two groups. Differences were considered significant if p-values were 0.05 or less.

Online supplemental materials. Fig. S1 shows Aire-expressing cells in adult and embryonic thymi. Fig. S2 shows altered morphology together with the distribution of GFP+ Aire-less mTECs in *Aire^-/-* mice. Fig. S3 shows altered morphology together with the distribution of GFP+ Aire-less mTECs in *Aire^-/-* mice expressing the nonautoreactive OT-II TCR transgene. Fig. S4 shows altered morphology of GFP+ Aire-less mTECs in *Aire^-/-* mice at neonatal stage P1. Table S1 shows detailed information for mice analyzed for involucrin-expressing mTECs. Online supplemental material is available at http://www.jem.org/cgi/content/full/jem.20080046/DC1.

REFERENCES

1. Kamradt, T., and N.A. Mitchison. 2001. Tolerance and autoimmunity. *N. Engl. J. Med.* 344:655–664.
2. Björses, P., J. Aaltonen, N. Horelli-Kuitunen, M.L. Yaspo, and I. Peltonen. 1998. Gene defect behind APECED: a new clue to autoimmunity. *Hum. Mol. Genet.* 7:1547–1553.
3. Pitkänen, J., and P. Peterson. 2003. Autoimmune regulator: from loss of function to autoimmunity. *Genes Immun.* 4:12–21.
4. Björses, P., M. Pelto-Huikko, J. Kaukonen, J. Aaltonen, I. Peltonen, and I. Ulmanen. 1999. Localization of the APECED protein in distinct nuclear structures. *Hum. Mol. Genet.* 8:259–266.
5. Heino, M., P. Peterson, J. Kudoh, K. Nagamine, A. Lagerstedt, V. Ovod, A. Ranki, I. Rantala, M. Nieminen, J. Tuukkanen, et al. 1999. Autoimmune regulator is expressed in the cells regulating immune tolerance in thymus medulla. *Biochem. Biophys. Res. Commun.* 257:821–825.
6. Hogquist, K.A., T.A. Baldwin, and S.C. Jameson. 2005. Central tolerance: learning self-control in the thymus. *Nat. Rev. Immunol.* 5:772–782.
7. Kyewski, B., and L. Klein. 2006. A central role for central tolerance. *Annu. Rev. Immunol.* 24:571–606.
8. Derbinski, J., A. Schulte, B. Kyewski, and L. Klein. 2001. Promiscuous gene expression in medullary thymic epithelial cells mirrors the peripheral self. *Nat. Immunol.* 2:1032–1039.
9. Anderson, M.S., E.S. Venanzi, L. Klein, Z. Chen, S.P. Berzins, S.J. Turley, H. von Boehmer, R. Bronson, A. Dierich, C. Benoist, and D. Mathis. 2002. Projection of an immunological self shadow within the thymus by the aire protein. *Science.* 298:1395–1401.
10. Derbinski, J., J. Gabler, B. Brors, S. Tierling, S. Jonnakuty, M. Hergenhahn, L. Peltonen, J. Walter, and B. Kyewski. 2005. Promiscuous gene expression in thymic epithelial cells is regulated at multiple levels. *J. Exp. Med.* 202:33–45.
11. Liston, A., D.H. Gray, S. Lesage, A.L. Fletcher, J. Wilson, K.E. Webster, H.S. Scott, R.L. Boyd, L. Peltonen, and C.C. Goodnow. 2004. Gene dosage–limiting role of *Aire* in thymic expression, clonal deletion, and organ-specific autoimmunity. *J. Exp. Med.* 200:1015–1026.
12. Kuroda, N., T. Mitani, N. Takeda, N. Ishimaru, R. Arakaki, Y. Hayashi, Y. Bando, K. Izumi, T. Takahashi, T. Nomura, et al. 2005. Development

of autoimmunity against transcriptionally unrepressed target antigen in the thymus of Aire-deficient mice. *J. Immunol.* 174:1862–1870.

13. Niki, S., K. Oshikawa, Y. Mouri, F. Hirota, A. Matsushima, M. Yano, H. Han, Y. Bando, K. Izumi, M. Matsumoto, et al. 2006. Alteration of intra-pancreatic target-organ specificity by abrogation of Aire in NOD mice. *J. Clin. Invest.* 116:1292–1301.

14. Anderson, M.S., E.S. Venanzi, Z. Chen, S.P. Berzins, C. Benoist, and D. Mathis. 2005. The cellular mechanism of Aire control of T cell tolerance. *Immunity.* 23:227–239.

15. Devoss, J., Y. Hou, K. Johannes, W. Lu, G.I. Liou, J. Rinn, H. Chang, R. Caspi, L. Fong, and M.S. Anderson. 2006. Spontaneous autoimmunity prevented by thymic expression of a single self-antigen. *J. Exp. Med.* 203:2727–2735.

16. Matsumoto, M. 2007. Transcriptional regulation in thymic epithelial cells for the establishment of self tolerance. *Arch. Immunol. Ther. Exp. (Warsz.).* 55:27–34.

17. Gillard, G.O., and A.G. Farr. 2006. Features of medullary thymic epithelium implicate postnatal development in maintaining epithelial heterogeneity and tissue-restricted antigen expression. *J. Immunol.* 176:5815–5824.

18. Gillard, G.O., J. Dooley, M. Erickson, L. Peltonen, and A.G. Farr. 2007. Aire-dependent alterations in medullary thymic epithelium indicate a role for Aire in thymic epithelial differentiation. *J. Immunol.* 178:3007–3015.

19. Gillard, G.O., and A.G. Farr. 2005. Contrasting models of promiscuous gene expression by thymic epithelium. *J. Exp. Med.* 202:15–19.

20. Moriguchi, T., M. Hamada, N. Morito, T. Terunuma, K. Hasegawa, C. Zhang, T. Yokomizo, R. Esaki, E. Kuroda, K. Yoh, et al. 2006. MafB is essential for renal development and F4/80 expression in macrophages. *Mol. Cell. Biol.* 26:5715–5727.

21. Niwa, H., K. Araki, S. Kimura, S. Taniguchi, S. Wakasugi, and K. Yamamura. 1993. An efficient gene-trap method using poly A trap vectors and characterization of gene-trap events. *J. Biochem.* 113:343–349.

22. Fuchs, E. 1990. Epidermal differentiation. *Curr. Opin. Cell Biol.* 2:1028–1035.

23. Hale, L.P., and M.L. Markert. 2004. Corticosteroids regulate epithelial cell differentiation and Hassall body formation in the human thymus. *J. Immunol.* 172:617–624.

24. Patel, D.D., L.P. Whichard, G. Radcliff, S.M. Denning, and B.F. Haynes. 1995. Characterization of human thymic epithelial cell surface antigens: phenotypic similarity of thymic epithelial cells to epidermal keratinocytes. *J. Clin. Immunol.* 15:80–92.

25. Maemura, K., Y. Yanagawa, K. Obata, T. Dohi, Y. Egashira, Y. Shibayama, and M. Watanabe. 2006. Antigen-presenting cells expressing glutamate decarboxylase 67 were identified as epithelial cells in glu-

tamate decarboxylase 67-GFP knock-in mouse thymus. *Tissue Antigens.* 67:198–206.

26. Hamazaki, Y., H. Fujita, T. Kobayashi, Y. Choi, H.S. Scott, M. Matsumoto, and N. Minato. 2007. Medullary thymic epithelial cells expressing Aire represent a unique lineage derived from cells expressing claudin. *Nat. Immunol.* 8:304–311.

27. Gray, D., J. Abramson, C. Benoist, and D. Mathis. 2007. Proliferative arrest and rapid turnover of thymic epithelial cells expressing Aire. *J. Exp. Med.* 204:2521–2528.

28. Senoo, M., F. Pinto, C.P. Crum, and F. McKeon. 2007. p63 Is essential for the proliferative potential of stem cells in stratified epithelia. *Cell.* 129:523–536.

29. Akiyoshi, H., S. Hatakeyama, J. Pitkänen, Y. Mouri, V. Doucas, J. Kudoh, K. Tsurugaya, D. Uchida, A. Matsushima, K. Oshikawa, et al. 2004. Subcellular expression of autoimmune regulator (AIRE) is organized in a spatiotemporal manner. *J. Biol. Chem.* 279:33984–33991.

30. Rossi, S.W., M.Y. Kim, A. Leibbrandt, S.M. Parnell, W.E. Jenkinson, S.H. Glanville, F.M. McConnell, H.S. Scott, J.M. Penninger, E.J. Jenkinson, et al. 2007. RANK signals from CD4+3− inducer cells regulate development of Aire-expressing epithelial cells in the thymic medulla. *J. Exp. Med.* 204:1267–1272.

31. Liu, Y.J. 2006. A unified theory of central tolerance in the thymus. *Trends Immunol.* 27:215–221.

32. Murata, T., K. Furushima, M. Hirano, H. Kiyonari, M. Nakamura, Y. Suda, and S. Aizawa. 2004. *ang* is a novel gene expressed in early neuroectoderm, but its null mutant exhibits no obvious phenotype. *Gene Expr. Patterns.* 5:171–178.

33. Yagi, T., T. Tokunaga, Y. Furuta, S. Nada, M. Yoshida, T. Tsukada, Y. Saga, N. Takeda, Y. Ikawa, and S. Aizawa. 1993. A novel ES cell line, TT2, with high germline-differentiating potency. *Anal. Biochem.* 214:70–76.

34. Tamamaki, N., Y. Yanagawa, R. Tomioka, J. Miyazaki, K. Obata, and T. Kaneko. 2003. Green fluorescent protein expression and colocalization with calretinin, parvalbumin, and somatostatin in the GAD67-GFP knock-in mouse. *J. Comp. Neurol.* 467:60–79.

35. Barnden, M.J., J. Allison, W.R. Heath, and F.R. Carbone. 1998. Defective TCR expression in transgenic mice constructed using cDNA-based alpha- and beta-chain genes under the control of heterologous regulatory elements. *Immunol. Cell Biol.* 76:34–40.

36. Kusser, K.L., and T.D. Randall. 2003. Simultaneous detection of EGFP and cell surface markers by fluorescence microscopy in lymphoid tissues. *J. Histochem. Cytochem.* 51:5–14.

37. Kajiura, F., S. Sun, T. Nomura, K. Izumi, T. Ueno, Y. Bando, N. Kuroda, H. Han, Y. Li, A. Matsushima, et al. 2004. NF-κB-inducing kinase establishes self-tolerance in a thymic stroma-dependent manner. *J. Immunol.* 172:2067–2075.